POLITECNICO
MILANO 1863

SCUOLA DI INGEGNERIA INDUSTRIALE
E DELL'INFORMAZIONE

EXECUTIVE SUMMARY OF THE THESIS

Experimental study of thermo-responsive polymer hydrogel systems for controlled drug release

TESI MAGISTRALE IN CHEMICAL ENGINEERING – INGEGNERIA CHIMICA

Author: CLAUDIA CERDÁN FLORES

Advisor: PROF. FILIPPO ROSSI

Co-advisor: ELISA LACROCE

Academic year: 2021-2022

1. Introduction

Hydrogels are cross-linked three-dimensional networks of water-soluble polymers, commonly used in clinical practices and experimental medicine for tissue engineering, regenerative medicine, diagnostics, or cell immobilization. The physical properties of hydrogels are precisely those that have aroused interest in their use in controlled drug release [1]. Their ability to swell in an aqueous environment and their porosity is what allows them to load the drug in the gel matrix and its subsequent release. The aim of this thesis is to characterize the behavior and structure of both the organic nanoparticles and the hydrogel, and the NP-gel system. In addition, to determine the efficiency of the system at temperatures higher than the LCST of the copolymer that constitutes the nanoparticles.

1.1. HPMC based hydrogels

Self-assembly of functional materials due to non-covalent intermolecular interactions provides moldable, reversible and therefore injectable hydrogels [2]. One of the most recently studied hydrogels of this type is the one that appears in the study by Appel et al. [4] in which an injectable shear-thinning supramolecular polymer-nanoparticle (PNP) hydrogel is synthesized, made from a mixture of dodecyl-modified hydroxypropyl methylcellulose ($HPMC_{12}$) and core-shell nanoparticles. HPMC was chosen for this thesis as the main polymer due to its high solubility, molecular weight, functionality and biocompatibility. The nanoparticles used were obtained from a copolymer based on polyNIPAm, which allowed them to be encapsulated as hydrophilic molecules in the bulk of the hydrogel, and also allowed to load the nanoparticles with hydrophobic molecules [3]. In this study the molecule loaded in the nanoparticles was Fluorescein isothiocyanate (FITC) as drug simulator.

1.2. Nanoparticles based on polyNIPAm

Cancer cells have a lower pH than that of the extracellular fluid, so that the nanoparticles can vary their pH when they come into contact with said cells from 7,4 to 5 via cellular proton effect [4]. Poly(N-isopropylacrylamide) (PNIPAm) is a water-soluble and hydrophilic polymer, which presents an extended chain conformation below 32 ºC, its LCST [4]. When its LCST is exceeded, PNIPAm undergoes a phase transition, which leads to a change in its structure, becoming a

hydrophobic polymer [5]. Combined with hydrophobic segments can form micellar core-shell structures below the LCST of PNIPAm. This combination creates a hydrophilic shell formed by the hydrated PNIPAm and a hydrophobic interior with the added groups [5]. In addition, the interior of the formed nanoparticles can be loaded with hydrophobic drugs, while the outer shell gives them stability in water and thermo-responsive properties [5]. In this thesis work, the synthesized nanoparticles were of poly(D, L-lactide)-g-poly N - isopropylacrylamide-co-methacrylic acid), following the experimental study by Lo et al. [5].

2. Materials

The list of the materials used for the nanoparticles synthesis is the following: D,L-Lactide (Sigma Aldrich), Benzyl alcohol (Sigma Aldrich), Stannous octoate ($Sn(Oct)_2$, Sigma Aldrich), Toluene (Sigma Aldrich), Triethylamine (TEA, Sigma Aldrich), Methacryloyl chloride (MACl, Sigma Aldrich), Methacrylic acid (MA, Sigma Aldrich), N-Isopropylacrylamide (NIPAm, Sigma Aldrich), 2,2'-Azobis(2-,methylpropionitrile) (AIBN, Sigma Aldrich), Acetone (Sigma Aldrich), Diethyl ether (Sigma Aldrich), Dichloromethane (DCM, Sigma Aldrich), Hexane (Sigma Aldrich), and Dimethyl sulfoxide (DMSO, Sigma Aldrich). And the list of the materials used for the HPMC-C_{12} synthesis and drug loading, is the following one: Hydroxypropyl methyl cellulose (HPMC, Sigma Aldrich), 1-dodecyl isocyanate (Sigma Aldrich), Triethylamine (TEA, Sigma Aldrich), N-methyl pyrrolidone (NMP, Sigma Aldrich), Acetone (Sigma Aldrich), Fluorescein isothiocyanate (FITC, Sigma Aldrich), Dimethyl sulfoxide (DMSO, Sigma Aldrich), and Hydrochloric acid (HCl, Sigma Aldrich).

3. Reference formulations

3.1. PLA-g-P(NIPAm-co-MAA) nanoparticles

For the synthesis of poly(D,L-lactide)-g-poly(N-isopropyl acrylamide-co-methacrylic acid), three consecutive reactions previously defined by Lo et al. [3] were performed.

3.1.1. Synthesis of polylactic acid (PLA) from D,L-Lactide

Table 1. Detailed recipe for the synthesis of PLA

Compound	g	eq	mL
D,L-Lactide	3,22	13	-
Benzyl alcohol	0,18	1	0,0172
$Sn(Oct)_2$	0,0035	0,005	-
Toluene	34,8	228,3	40

To prepare the reaction, a two-neck flask was used, and 3,22 g of D,L-Lactide were placed on it. Then, 40 mL of toluene were added under a continuous flow of nitrogen and the mixture was stirred in an oil bath at 130 ºC. Afterwards, 0,0035 g of stannous octoate were added with 0,172 mL of benzyl alcohol and the mixture went under stirring and under nitrogen for 4 hours at 130 ºC. Then, a purification step was done with 50 mL of previously freeze diethyl ether placed in a flask, and dropping the reaction product inside it. A precipitate was formed. The liquid part was recovered and the precipitate was dried under vacuum.

3.1.2. Synthesis of Polylactic Acid Methacrylate (PLA-MA)

Table 2. Detailed recipe for the synthesis of PLA-MA

Compound	g	eq	mL
PLA	1,09	1	-
Triethylamine	0,33	2,97	0,454
Methacryloyl chloride	0,28	2,47	0,261
Anhydrous toluene	-	-	50

1,09 g of PLA were transferred to a 3-neck balloon flask and dried on the rotary evaporator. Anhydrous toluene was then added to the balloon flask on ice, at 0°C and under a continuous flow of nitrogen. TEA and methacryloyl chloride were also added, always under nitrogen flow. After all reagents were added, the reaction was left running overnight at room temperature under nitrogen atmosphere. Then, a purification step was necessary doing first an extraction with DCM and distilled water, and followed by a precipitation with DCM and hexane. The extraction was done with 10 mL of DCM and 15 mL of distilled water using a separator. The precipitation was done to remove the

methacryloyl chloride from the organic phase. 3 mL of DCM were used to dissolve the organic phase, and this solution was dropped in a flask with previously freeze 100 mL of hexane. A precipitate was formed and dried under vacuum.

3.1.3. Synthesis of PLA-g-P(NIPAm-co-MAA) graft copolymer

Table 3. Detailed recipe for the synthesis of PLA-g-P(NIPAm-co-MAA)

Compound	mg	eq	mL
PLA-MA	90,54	3,3	-
Methacrylic Acid	20,22	8,7	0,0199
NIPAm	268,86	88	-
AIBN	4,47	1	-

90,54 mg of PLA-MA were dissolved in DCM and dried in a rotary evaporator in a three-necked balloon flask. Once dried, 5,3 mL of acetone, the methacrylic acid and the NIPAm were added to the flask, under a continuous flow of nitrogen and a temperature of 70 ºC. Then 4,47 mg of AIBN, which was the initiator of the reaction, were dissolved in 1 mL of acetone. The solution was added to the flask with a syringe, always under a continuous flow of nitrogen. Four hours later other 20 mL of acetone were added and the reaction went for 24 hours at 70°C and under nitrogen. Also a purification step was done by dropping the reaction product into a previously freeze 150 mL of diethyl ether. A precipitate was formed. The liquid was recovered and the precipitate was dried under vacuum.

3.1.4. Organic nanoparticles preparation

To obtain the nanoparticles, a dialysis was prepared. To do it, the already purified copolymerization product (PLA-g-P(NIPAm-co-MAA)) was dissolved in 25 mL of dimethyl sulfoxide (DMSO). The membrane used was a cellulose membrane with a molecular weight cut-off of 14000 Da. To prepare it, the membrane was soaked in distilled water and filled with the DMSO solution, closed and immersed in a distilled water bath with stirring for 48 hours. Once the 48 hours have elapsed, the solution obtained was frozen and lyophilized to obtain the nanoparticles.

3.2. HPMC-C_{12} hydrogel

The reaction for the HPMC functionalization was performed following a previous study from Grosskopf et al. [4].

Table 4. Detailed recipe for the HPMC-C_{12} synthesis

Compound	g	eq	mL
HPMC	1	1	-
1-dodecyl isocyanate	0,105	50	0,120
Triethylamine	-	-	2 drops
N-methylpyrrolidone	-	-	50

To perform the functionalization of the HPMC-C_{12}, 1 g of HPMC need to be dissolved in 45 mL of N-methylpyrrolidone by stirring at 80 ºC for, approximately, 2 hours. Once the solution has reached the room temperature, a solution of 0,120 mL of 1-dodecyl isocyanate with 2 drops of TEA was dissolved in 5 mL of NMP. This solution was then added to the reaction mixture, which was stirred at room temperature overnight. Then, purification was done by dropping the solution into a flask with previously cooled acetone. The solution was filtered, and the polymer obtained was dried under vacuum and left with distilled water under stirring for a night. A dialysis was then performed using a cellulose membrane with a molecular weight cut-off of 14000 Da. The membrane was soaked in distilled water and filled with the solution, closed and immersed in a distilled water bath with stirring for 24 hours. Then it was frozen and lyophilized.

3.3. Drug release from polymer-nanoparticles HPMC based hydrogel

The drug release from polymer-nanoparticles hydrogel consists of three steps: the preparation of the HPMC solution, the solution of nanoparticles, and gel preparation.

- HPMC-C_{12} solution

After the lyophilization, 240 mg of HPMC-C_{12} were dissolved in 4 mL of distilled water for 48 hours in the shaker to obtain the gel. Afterwards, the gel was transferred into a 5 mL syringe. Then, 0,33 g of the gel were transferred from the 5 mL syringe to a 1 mL syringe.

- Nanoparticles solution

To prepare the nanoparticles solution, 40 mg of nanoparticles were dissolved in 1,566 mL of

distilled water. After that, 100 µL of a solution of FITC in DMSO with a concentration of 28,8 mg/mL were taken and added to the solution of the nanoparticles. This solution went under stirring for 25 minutes. 500 µL of this solution were transferred into a 1 mL syringe.

- Gel preparation

To mix the two solutions, both syringes were joined with a connector and 60 cycles were carried out. This process was carried out in three different syringes and three membranes were prepared.

4. Results and discussion

4.1. PLA-g-P(NIPAm-co-MAA) nanoparticles characterization

To characterize the synthesized nanoparticles, different analysis were performed at each stage, such as ^{1}H-NMR spectra, DLS or AFM analysis for the final nanoparticles. In each step the correct development of the synthesis was verified, and the final characterization of the nanoparticles after the dialysis is explained below:

4.1.1. ^{1}H-NMR analysis

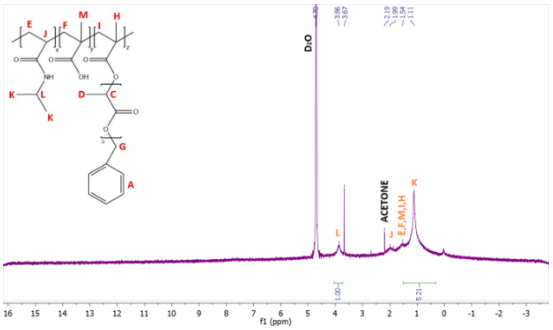

Figure 1. ^{1}H-NMR analysis of PLA-g-P(NIPAm-co-MAA) nanoparticles after dialysis in distilled water

What is observed in this spectrum is that, after dialysis, the peaks corresponding to the hydrophobic chains no longer appear. This fact confirms the successful formation of nanoparticles with hydrophobic terminal groups facing inwards, and hydrophilic terminal groups facing outwards (Figure 1).

4.1.2. DLS analysis

According to the literature studied, as the temperature increases, a decrease in the size of the particles should be expected, since they have a thermo-responsive behavior. A DLS analysis was performed analyzing the samples at 37 ºC and 42 ºC. They were analyzed three times and the results obtained are reported in Table 5:

Table 5. Single DLS analysis for 37 ºC and 42 ºC

T (ºC)	Average Size (d.nm)	Standard Deviation (d.nm)
37	**2003,33**	388,40
42	**1316,33**	213,63

As can be observed, in this experiment, a notable change in particle size is shown as a function of temperature, decreasing approximately 700 nm between 37 ºC and 42 ºC.

4.2. HPMC-C$_{12}$ hydrogel characterization

For the HPMC-C$_{12}$ hydrogel characterization, a FT-IR and a SEM analysis within some rheology tests, with and without nanoparticles were performed.

4.2.1. FT-IR analysis

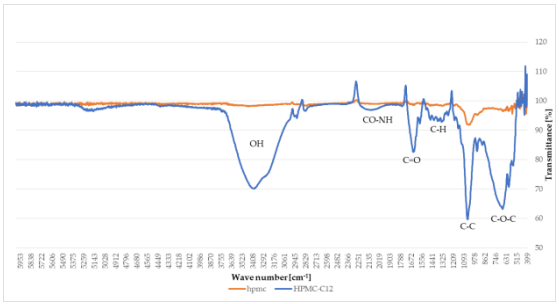

Figure 2. FT-IR spectrum for HPMC and HPMC-C$_{12}$ comparison

As observed in Figure 40, there are some significant peaks to be analysed. OH peak: around 3400 cm^{-1}, corresponds to the vibration and stretching of the –OH groups. CO-NH peak: around 1150 cm^{-1} is the corresponding to the CO-NH of the functionalized part of HPMC-C$_{12}$. C=O peak: characteristic absorption band of C=O bonds normally found around 1700-1650 cm^{-1}. C-H peak: found between 1400-1350 cm^{-1}, it represents the symmetrical vibration of C-H bonds, while the region between 1500-1450 cm^{-1} represents the asymmetric vibration out of phase of C-H bonds. C-C peak: found around 1000 cm^{-1}, characteristic of C-C bonds. C-O-C peak: at 650 cm^{-1}, characteristic of C-O-C bond of HPMC.

4.2.2. SEM analysis

The SEM analysis was performed for the HPMC-C_{12} with and without nanoparticles, shown in Figure 3 and Figure 4.

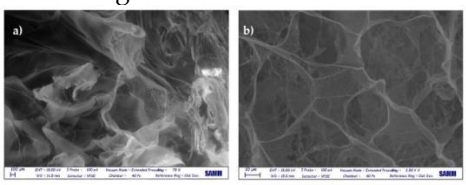

Figure 3. SEM images of HPMC-C_{12} hydrogel without NPs at: a) 100 µm; b): 10 µm

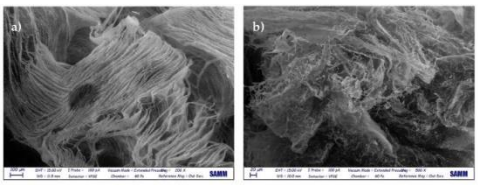

Figure 4. SEM images of HPMC-C_{12} hydrogel with NPs at: a) 100 µm; b): 20 µm

In the images of the SEM analysis obtained, the appearance and shape of the hydrogel could be observed at different microscope magnifications. The main difference was that before the nanoparticles were introduced, the surface of HPMC-C_{12} was smoother. When mixing the nanoparticles with the gel, these nanoparticles were observed in all magnifications as small spheres well adhered to the gel structure (Figure 3 and Figure 4).

4.2.3. Rheology tests

The most characteristic rheological test performed on the HPMC-C_{12} hydrogel was the amplitude sweep.

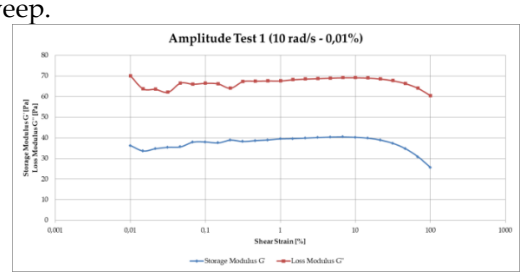

Figure 5. Amplitude sweep test (10 rad/s – 0,01 % minimum deformation)

As can be seen in the amplitude test carried out (Figure 5), the values of G'' are greater than those of G' throughout the test, it is known that the material does not behave like a gel, but like a solution. It can be observed a transition from a linear behavior to a non-linear one (Figure 5) starting from a 10% shear strain, but without any crossover that indicates the transition from a solid-like material to a liquid-like material.

4.3. Drug release from polymer-nanoparticles HPMC-C_{12} hydrogels

To verify the release efficiency of organic nanoparticles in HPMC-C_{12} hydrogels, a drug release experiment was carried out in which the amount of drug simulant (FITC) released in an acidic aqueous medium (pH 5) was measured at 42ºC. The absorbance was obtained by UV spectroscopy at 440 nm, and the percentage of drug released was defined as the ratio between the amount released and the total amount of drug loaded in the system.

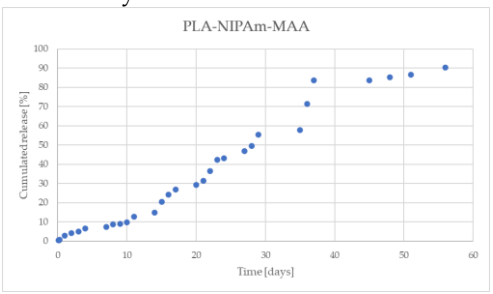

Figure 6. FITC release by PLA-g-P(NIPAm-co-MAA) nanoparticles at 42 °C in acidic environment (pH 5)

An increasing trend within the time can be observed in Figure 6, reaching a plateau at 90% of drug release from day 38. Such a high time to reach this value may be due to the interaction with hydrophobic core and the release in aqueous environment.

5. Conclusions

PLA-g-P(NIPAm-co-MAA) organic nanoparticles were synthesized and characterized, as well as the HPMC-C_{12} hydrogel by different analysis techniques. Regarding the organic nanoparticles, the synthesis consisted of three stages that were carried out until the copolymer PLA-g-P(NIPAm-co-MAA) was successfully obtained. Also the nanoparticles resulting from the dialysis of said copolymer were successfully obtained. Each of the steps of the synthesis process gave rise to a product that was analyzed by ^{1}H-NMR. Furthermore, after dialysis of the copolymer, an AFM analysis was also performed to obtain images of the synthesized nanoparticles, as well

as a DLS analysis to determine the variation of particle size with temperature. ^{1}H-NMR spectra confirmed the formation of the nanoparticles. DLS analysis resulted in an average nanoparticle size in the order of 2000 nanometers that was analyzed as a function of temperature. Samples of nanoparticles dissolved in an acidic aqueous medium at pH 5 at 37 ºC and 42 ºC were measured and a decrease in particle size was observed. On the other hand, the HPMC was functionalized to increase the interaction with the hydrophobic core of the nanoparticles. FT-IR analysis allowed obtaining the unique and characteristic IR spectrum of the HPMC-C_{12} hydrogel. Once the nanoparticles and the hydrogel had been characterized separately, by means of SEM analysis and rheological tests, the behavior of the system was verified. The main difference observed in SEM images was in the appearance of the gel surface, with the gel without nanoparticles being smoother and the nanoparticles adhering to the gel being easily observed once introduced. Regarding the rheological tests, an amplitude sweep test was performed. A value of G'' higher than that of G' was obtained throughout the test, so the solid-like behavior of the gel could not be confirmed, but rather a liquid-like behavior. The last tests carried out were those for the release of FITC as a mimetic drug from the hydrogel-nanoparticle system. In this case, the cumulative percentage of FITC released from the system at 42 ºC was analyzed, and a 90% of release was reached in 38 days. This is due to the presence of a hydrophobic molecule in a hydrophobic core in an aqueous solution. After all the studies were carried out, a series of tests are interested to carry out as a future plan to complete this study. First of all, a drug release experiment should be carried out to verify that the system works at 37 ºC, with the aim to compare it with the experiment done at 42 ºC and verify its thermo-responsiveness above 40 ºC; as well as to characterize the nanoparticles with the aim of verifying the LCST of the copolymer and their response when found in a medium at said temperature. Another future goal to keep in mind would be with respect to rheological tests, trying to increase the concentration of particles in the hydrogel to obtain a less liquid behavior, or add more crosslinking agents, always ensuring the good injectability of the system. Finally, once all these aspects of the hydrogel-nanoparticle system have been solved, the possibility of continuing the study with real drugs or increasing the temperature in the application to ensure efficient and successful localized drug release would be considered.

6. Acknowledgements

First of all, thanks to my advisor Prof. Filippo Rossi and my co-advisor Elisa Lacroce, for the opportunity to work on this very interesting project and for trusting on my work. To all the colleagues in the laboratory and to the entire scientific community who work every day on research projects as necessary as this one. And finally, to all the people who have accompanied me on this path.

References

[1]. Hoare, T. R., & Kohane, D. S. (2008). Hydrogels in drug delivery: Progress and challenges. *Hydrogels in drug delivery: Progress and challenges*, 49(8), 1993–2007.

[2]. Appel, E. A., Tibbitt, M. W., Webber, M. J., Mattix, B. A., Veiseh, O., & Langer, R. (2015). Self-assembled hydrogels utilizing polymer–nanoparticle interactions. *Nature Communications*, 6(1).

[3]. Grosskopf, A. K., Roth, G. A., Smith, A. A. A., Gale, E. C., Hernandez, H. L., & Appel, E. A. (2019). Injectable supramolecular polymer–nanoparticle hydrogels enhance human mesenchymal stem cell delivery. *Bioengineering & Translational Medicine*, 5(1).

[4]. Lo, C. L., Lin, K. M., & Hsiue, G. H. (2005). Preparation and characterization of intelligent core-shell nanoparticles based on poly(d,l-lactide)-g-poly(N-isopropyl acrylamide-co-methacrylic acid). *Journal of Controlled Release*, 104(3), 477–488.

[5]. Capella, V., Rivero, R.E., Liaudat, A.C., Ibarra, L.E., Roma, D.A., Alustiza, F., Mañas, F., Barbero, C.A., Bosch, P., Rivarola, C.R., & Rodriguez, N. (2019). Cytotoxicity and bioadhesive properties of poly-N-isopropylacrylamide hydrogel. *Heliyon*, 5(4).

POLITECNICO
MILANO 1863

SCUOLA DI INGEGNERIA INDUSTRIALE
E DELL'INFORMAZIONE

Experimental study of thermo-responsive polymer hydrogel systems for controlled drug release

TESI DI LAUREA MAGISTRALE IN
CHEMICAL ENGINEERING – INGEGNERIA CHIMICA

Author: **Claudia Cerdán Flores**

Student ID:	10785680
Advisor:	Filippo Rossi
Co-advisor:	Elisa Lacroce
Academic Year:	2021-22

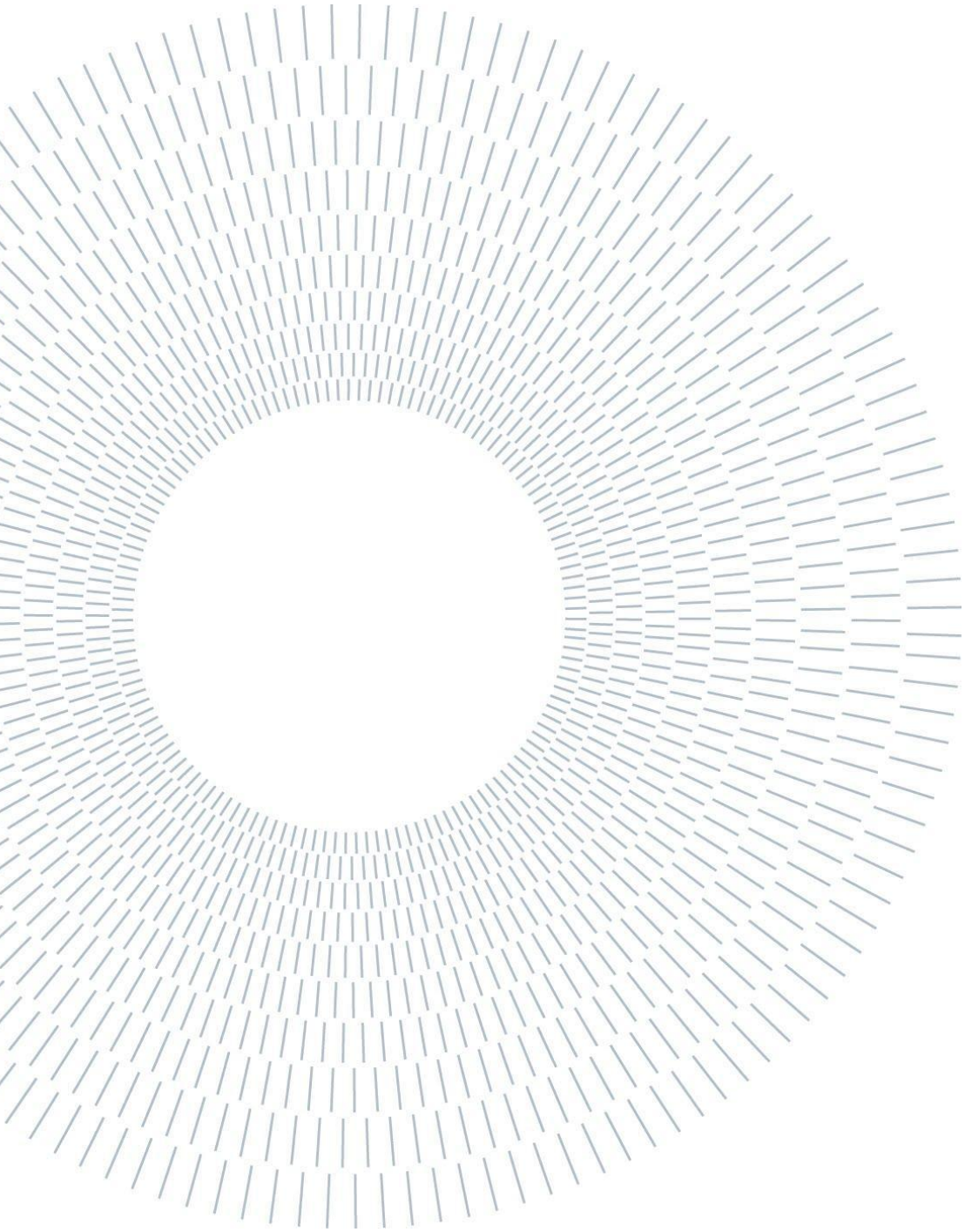

Abstract

In recent years, medicine has become interested in localized drug delivery systems for the treatment of diseases such as cancer. Drugs used in cancer treatment can be highly damaging to healthy tissues as well as to the regions where the disease is present, so a highly localized drug delivery system is very important.

In this context, systems for the localized controlled release of drugs activated by external stimuli such as pH and temperature have been investigated.

The peculiarity of NIPAm-based copolymers is that their lower critical solution temperature (LCST) can be modulated by varying the amounts of ionic copolymers present. So particles made from such copolymers can be used for temperature-sensitive drug delivery. In this work, the copolymer poly(D,L-lactide)-g-poly(N-isopropylacrylamide-co-methacrylic acid) (PLA-NIPAm-MAA) was produced following the procedure described by Lo et al. [26], from which organic nanoparticles with interesting properties in the field of drug delivery were obtained.

The obtained nanoparticles were encapsulated in a cellulose hydrogel, hydroxypropyl methylcellulose (HPMC), a hydrogel in which the hydroxyl groups are replaced by methyl and hydroxypropyl groups that give the HPMC gelation abilities. In addition, its swelling and thermal gelling properties make it a temperature-reversible gel. It is for this reason and for its biocompatibility that HPMC arouses great interest in pharmaceutical applications, specifically in the field of drug delivery.

The behavior and structure of both the organic nanoparticles and the hydrogel were studied and characterized using different analysis techniques such as ^{1}H-NMR spectroscopy, GPC, AFM microscopy, DLS, SEM and rheological tests.

The nanoparticles, loaded with fluorescein isothiocyanate (FITC) as a mimetic drug, were placed in the functionalized hydroxypropyl methylcellulose (HPMC-C_{12}) hydrogel and were immersed in an acidic aqueous solution (pH 5), because of the pH-responsiveness of methacrylic acid. In this case, the drug loaded in the particles is ejected outwards due to the compression of the particles and a swelling of the hydrogel, that occurs when the temperature of the system exceeds the LCST of the copolymer (37 ºC).

The nanoparticles-hydrogel system was also characterized and successively, a drug release experiment was performed to evaluate the amount of drug released over time by this type of system. The amount of FITC released was analyzed at 42 ºC.

From the experimental results, it will be determined if, in fact, the NP-gel system is more efficient at temperatures higher than the LCST of the copolymer that constitutes the nanoparticles and, in what proportion the amount of drug is released depending on the studied temperature.

Abstract in lingua italiana

Negli ultimi anni, la medicina si è interessata ai sistemi di somministrazione di farmaci localizzati per il trattamento di malattie come il cancro. I farmaci utilizzati nel trattamento del cancro possono essere altamente dannosi per i tessuti sani e per le regioni in cui è presente la malattia, quindi un sistema di somministrazione di farmaci altamente localizzato è molto importante.

In questo contesto sono stati studiati sistemi per il rilascio controllato di farmaci attivati da stimoli esterni come pH e temperatura.

La particolarità dei copolimeri a base NIPAm è che la loro lower critical solution temperature (LCST) può essere modulata variando le quantità di copolimeri ionici presenti. Quindi le particelle prodotte da tali copolimeri possono essere utilizzate per la somministrazione di farmaci sensibili alla temperatura. In questo lavoro, il copolimero poly(D,L-lactide)-g-poly(N-isopropylacrylamide-co-methacrylic acid) (PLA-NIPAm-MAA) è stato prodotto seguendo la procedura descritta da Lo et al. [26], da cui sono state ottenute nanoparticelle organiche con proprietà interessanti nel campo del drug delivery.

Le nanoparticelle ottenute sono state incapsulate in un idrogel di cellulosa, idrossipropilmetilcellulosa (HPMC), un idrogel in cui i gruppi ossidrile sono sostituiti da gruppi metilico e idrossipropilico che conferiscono le capacità di gelificazione dell'HPMC. Inoltre, le sue proprietà di rigonfiamento e gelificazione termica lo rendono un gel termoreversibile. È per questo motivo e per la sua biocompatibilità che HPMC suscita grande interesse nelle applicazioni farmaceutiche, in particolare nel campo del drug delivery.

Il comportamento e la struttura sia delle nanoparticelle organiche che dell'idrogel sono stati studiati e caratterizzati utilizzando diverse tecniche di analisi come la spettroscopia ^{1}H-NMR, GPC, microscopia AFM, DLS, SEM e test reologici.

Le nanoparticelle, caricate con isotiocianato di fluoresceina (FITC) come farmaco mimetico, sono state poste nell'idrogel di idrossipropilmetilcellulosa funzionalizzata (HPMC-C_{12}) e sono state immerse in una soluzione acquosa acida (pH 5), a causa della risposta alle variazioni del pH dell'acido metacrilico. In questo caso, il farmaco caricato nelle particelle viene espulso verso l'esterno a causa della compressione delle particelle e di un rigonfiamento dell'idrogel, che si verifica quando la temperatura del sistema supera l'LCST del copolimero (37 ºC).

È stato inoltre caratterizzato il sistema nanoparticelle-idrogel e successivamente è stato eseguito un esperimento di rilascio di farmaci per valutare la quantità di farmaco rilasciata nel tempo da questo tipo di sistema. La quantità di FITC rilasciata è stata analizzata a 42 ºC.

Dai risultati sperimentali si determinerà se, infatti, il sistema NP-gel è più efficiente a temperature superiori all'LCST del copolimero che costituisce le nanoparticelle e, in quale proporzione viene rilasciata la quantità di farmaco a seconda dell'analisi studiata temperatura.

Contents

1. Introduction

1.1 Hydrogels

Hydrogels are cross-linked three-dimensional networks of water-soluble polymers. They are commonly used in clinical practices and experimental medicine for tissue engineering, regenerative medicine, diagnostics, or cell immobilization, among other applications.

Hydrogels can be synthesized from any water-soluble polymer and encompass a wide range of chemical compositions and physical properties. These physical properties are precisely those that have aroused interest in their use in controlled drug release [1].

Their ability to swell in an aqueous environment and their porosity is what allows them to load the drug in the gel matrix and its subsequent release.

On the other hand, the biocompatibility of hydrogels is favoured by the large amount of water and the physical-chemical similarities with the extracellular matrix [1].

1.1.1 Network structure of hydrogels

The polymer chains in hydrogels are cross-linked by chemical or physical bonds forming a mesh. Chemical bonds are due to chemical reactions or strong bonds by radical polymerization, functional groups reacting with each other or high-energy radiation. Physical bonds are due to ionic, hydrophobic, or non-covalent interactions or thermo condensation, among others (Figure 1) [2]. These types of physical and chemical bonds may change the final properties of the hydrogels, which can be studied by different methods in order to characterise the polymer. Those methods are based on scattering, rheology, strength measurements,

composition determination and microscopy to obtain physical and chemical information.

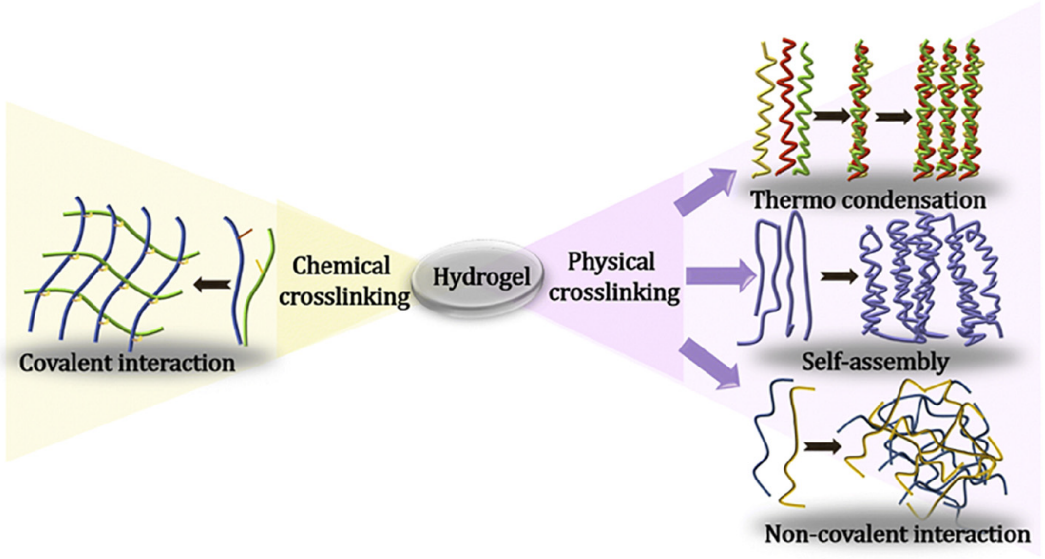

Figure 1: Schematic representation of the main crosslinking methods [2]

One of the most important parameters for the characterization of hydrogels is the determination of the local structure and morphology of the hydrogel.

The swelling ratio (SR) is the parameter that determines the water content, one of the most important parameters since the hydrogel is mainly composed of water (Equation 1). The swelling behaviour is related to the local structure of the hydrogel and is influenced by pH, ionic strength, and hydrophobicity [2].

$$Swelling\ Ratio\ (SR) = \frac{M_{wet} - M_{dry}}{M_{dry}} \qquad \text{[Equation 1]}$$

Being:

M_{wet} = mass of wet hydrogel

M_{dry} = mass of dry hydrogel

This equation is determined by comparing the hydrogel dry mass to the hydrogel wet mass.

The crosslinking density (CLD, mol/m^3) of the polymeric chains represents the number of interconnected polymeric chains per unit volume to form the local structure of the gel. The crosslinking density affects many properties of the hydrogel such as the shear modulus (G), the volumetric swelling ratio (Q) or the diffusion coefficient (D). This relationship between the CLD and these parameters with respect to the distance between sequential cross-linking points (ξ), is represented in (Figure 2) [2, 3]:

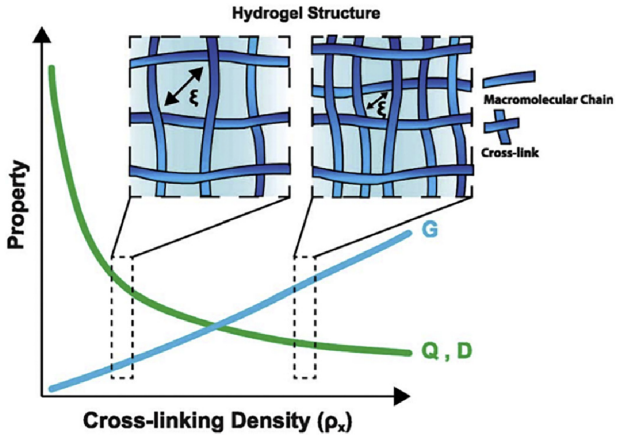

Figure 2: Scheme of the hydrogel properties relationship with the CLD [2]

According to Figure 2, low and high cross-linking densities have different mesh size (ξ), which has relationship with the hydrogel properties of shear modulus (G), equilibrium swelling ratio (Q) and diffusivity (D).

The CLD is obtained from the Flory-Rehner equation, which defines the swelling equilibrium of the hydrogel (Equation 2). This equation defines the swelling behaviour of hydrogels since the swelling of the hydrogel increases with the CLD of the polymer chains:

$$\rho_x = \frac{-\ln ln\left(1-V_r\right)+V_r+\chi V_r^2}{V_s\left(V_r^{\frac{1}{3}}-0{,}5V_r\right)} \qquad \text{[Equation 2]}$$

Being:

ϱ_x = crosslinking density of the polymeric chains

V_s = molar volume of solvent

χ = Flory-Huggins polymer-solvent interaction parameter

V_r = volume of hydrogel in the equilibrium swollen state, defined as:

$$V_r = \frac{\frac{m_1}{\rho_1}}{\frac{m_1}{\rho_1}+\frac{m_2}{\rho_2}} \qquad \text{[Equation 3]}$$

Being:

m_1 = weight of dry polymer

ϱ_1 = density of dry polymer

m_2 = weight of solvent in the swollen sample

ϱ_2 = solvent density

Mesh size in regenerative medicine must be determined under realistic conditions. Therefore, when determining mesh size in real systems, the volume of hydrogel in the swollen equilibrium state must be determined in the physiological solution in which the gel is swollen, according to (Equation 3) [4].

1.1.2 Swelling behaviour of hydrogels

One of the main properties of hydrogels is their ability to swell when in contact with a thermodynamically compatible solvent. When the hydrogel in its initial state comes into contact with the solvent, the solvent attacks the hydrogel surface penetrating the polymeric matrix [5].

It is thanks to the swelling of the gel that the encapsulation and release of the drug and the particles become possible (Figure 3) [2].

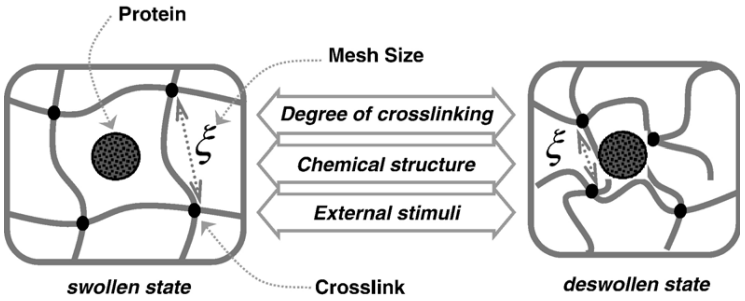

Figure 3: Representation of the swelling behaviour of a hydrogel as a function of mesh size [6]

An increase in the concentration of the crosslinking agent leads to an increase in the crosslinking density, so it will also influence the swelling capacity, decreasing it [7].

The swelling rate of hydrogels is one of the most important characteristics of swelling. The swelling rate is determined by different physical-chemical parameters such as the degree of porosity and the type of porous structure.

Depending on the size of the pore, they can be classified into four types [5]:

- Non-porous hydrogels: 10 – 100 Å

They are characterized by having very densely packed polymeric chains and because solute transport is highly limited by diffusion through free holes.

- Microporous hydrogels: 100 – 1000 Å

In this type of hydrogels, solute transport is due to a combination of both molecular diffusion and convection in the water-filled pores. This behaviour is due to the fact that the pore size begins to resemble the size of the diffusing solutes.

- Macroporous hydrogels: 0,1 – 1 μm

The pore size of macroporous hydrogels is already much larger than the diffusing solute, so in this case the transport is due to a diffusion phenomenon. The effective solute diffusion coefficient (D_{eff}) can be related to the solute diffusion coefficient in water (D_{iw}), the partition coefficient (K_p), the mesh size (ξ) and the tortuosity (τ), according to the following equation (Equation 4):

$$D_{eff} = D_{iw} \frac{K_p \xi}{\tau}$$ [Equation 4]

- Superporous hydrogels: range of several hundred μm

Due to the large size of the pores, swelling by water absorption is carried out rapidly by capillarity rather than by simple absorption. This rapid swelling causes weak mechanical properties in its structure [5].

1.1.3 Drug loading and delivery

Hydrogels are often used for controlled drug release due to their biocompatibility and hydrophilic characteristics. It is also possible to control the rate of drug release by modifying some important parameters such as swelling or crosslinking density, in order to adjust the drug release schedule [8]. The importance of the injectability of the hydrogel should be highlighted, since this would lead to less anatomical invasion, as well as avoiding unnecessary risks due to surgical interventions.

Biocompatibility is due to the high water content in the hydrogels and the similarity of hydrogels to the native extracellular matrix, both mechanically and compositionally [1].

As far as the loading of the drug in the hydrogel structure is concerned, there are two main methods [9]. The first one consists of a polymerization reaction with the hydrogel monomer, an initiator, the drug and the presence, or not, of a crosslinking agent, which entails trapping the drug directly in the hydrogel matrix. In contrast, in the second method, the hydrogel is first synthesized and allowed to reach swelling equilibrium in a solution already containing the drug, followed by drying to obtain the drug-hydrogel system [9].

The rate of release depends on two phenomena: the relaxation of macromolecular chains and diffusion. When the system is hydrophilic, the polymer hydrogel swells progressively, which leads to important structural changes that lead to the relaxation of the macromolecular chains and the alteration of the shape and size of the pores that, in turn, will cause changes in the tortuosity of the network during

dilation, leading to drug release by diffusion, which will occur through the water-filled pores as well as through the swollen polymer [10].

In order to characterize both types of diffusion, Korsmeyer and Peppas [10] introduced an equation that represents the fraction of drug released as a function of time, according to the following expression (Equation 5):

$$\frac{M_t}{M_\infty} = k\, t^n \qquad \text{[Equation 5]}$$

Being:

M_t = mass released at time t

M_∞ = mass released at time t ∞

k = kinetic constant characteristic of the drug-polymer system

n = release exponent depending on the mechanism of release

Drug release from the interior of the hydrogel consists of initial water absorption and the subsequent release by diffusion, governed by Fick's law. The Fickian behaviour of the release will be given by the value of the release exponent, n.

- **n = 0,5**: the release follows a Fickian behaviour
- **0,5 < n < 1**: the release is considered anomalous (non-Fickian diffusion)
- **n = 1**: Case II transport (in this case, the behaviour of the release will be of order 0, and it will be a desirable mechanism because it will be time independent) [10]

An important fact is that Equation 5 defined by Korsmeyer and Peppas is only valid up to 70% of released mass [3].

In conclusion, the release rate can be modulated and, together with the high biocompatibility, is what makes hydrogels so widely used in the medical field.

1.1.4 Influence of environmental conditions

Hydrogels are capable of containing up to 99% of their mass in water and, thanks to this property, they are able to swell and shrink when the amount of water in the polymer network changes, which can occur in response to different external stimuli such as temperature, pH or ionic strength, among others [11]. Among the most studied hydrogels in pharmaceutical applications are those that respond to changes in pH and/or temperature and, for this reason, have been widely used in the development of drug delivery systems [12].

There are many reports that study both types of hydrogels, such as [11]:

- pH-responsive: systems based on polyelectrolytes.
- Thermo-responsive: polymer-based systems with lower or upper critical solution temperature, LCST and UCST, respectively.

In all cases, both the application and the removal of said external stimuli lead to deformation and relaxation of the hydrogel. That means, those hydrogels subject to changes with the surrounding environment have the ability to change from solution to gel when an external stimulus is applied (Figure 4).

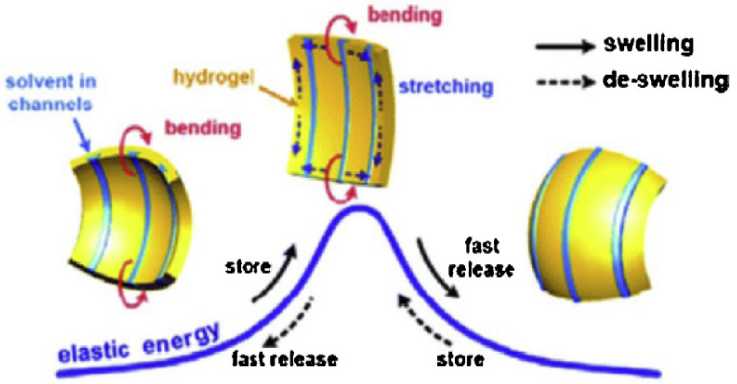

Figure 4: Representation of the expansion and contraction of a hydrogel caused by external stimuli [11]

1.1.4.1 Thermo-responsive hydrogels

The sensitivity of some hydrogels to changes in the temperature of their environment makes them highly useful hydrogels for the transition from solution to gel (sol-gel transition), since temperature will be the only stimulus to be modified [13].

The sol-gel transition is characterized by drastic changes in the viscoelastic properties of the polymer structure [14].

Some hydrogels separate the solution phase from the gel phase by a certain temperature, the lower critical solution temperature (LCST), below which the polymer is soluble and, as it overcomes the LCST barrier, it becomes more hydrophobic and insoluble, becoming a gel [13]. On the contrary, it occurs with those hydrogels that have been synthesized by cooling a solution polymer, the sol-gel limit of these is the upper critical solution temperature (UCST), above which the components of a mixture are miscible in all proportions.

To explain the hydrophobic effect of polymers whose limit temperature is the LCST, the Gibbs free energy expression is used (Equation 6):

$$\Delta G = \Delta H - T\Delta S \qquad \text{[Equation 6]}$$

When a polymer is dissolved in water, three types of interactions take place:

- Between polymer molecules
- Between polymer and water
- Between water molecules

An increase in temperature above the LCST results in a negative value of the free energy of the system, which makes the interaction of water and polymer unfavourable, thus facilitating the other two types of interactions. This negative value of free energy is attributed to a much higher value of the entropy term than the enthalpy one, and this is due to the fact that the entropy increases thanks to the interaction between the water molecules that govern the system [13].

All these changes result in a reversible physical union of the polymeric chains, which means that the polymer can become soluble again as soon as the external stimulus, in this case temperature, stops.

1.1.4.2 pH-responsive hydrogels

The degree of swelling of some hydrogels is subject to changes in response to variations in environmental conditions. Those hydrogels sensitive to changes in the pH of the medium can be synthesized from copolymerization reactions of ionizable electrolytes. This would lead to a change in the ionization of the electrolyte and, therefore, a change in the swelling capacity of the hydrogel [15].

To study the swelling behaviour of these hydrogels, the pH of the medium and the pK_a values of the acidic component of the polymer are essential [16].

The pH values can influence swelling in different ways:

- An acid pH favors swelling in basic polymers
- A basic pH favors swelling in acidic polymers

This is due to the repulsion between ions with the same charge:

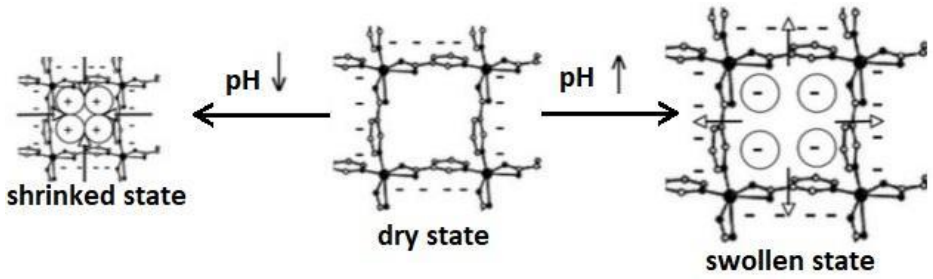

Figure 5: pH effect on acid hydrogels [16]

Those polymers with pK_a values between 3 and 10 are good options for systems sensitive to changes in pH. Weak acids such as carboxylic acids and phosphoric acid, and bases such as amines, change their ionization state as the pH varies, leading to changes in the swelling behaviour of hydrogels when these ionizable groups cross-link to the polymer structure [17].

1.1.5 Classification of hydrogels

There are many classification criteria for hydrogels. They depend on their physical properties, the nature of swelling, preparation methods or ionic charges, among others, as can be seen in Fig. 6 [18, 19]:

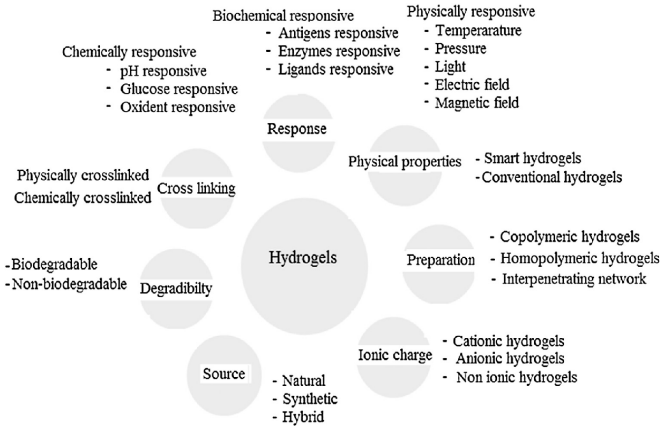

Figure 6: Classification of hydrogels based on different properties [18]

Based on source, hydrogels can be:

- Natural
- Synthetic

1.1.5.1 Classification based on preparation method

This classification is explained according to the polymeric composition of the hydrogel and, depending on the method used to prepare it, three types of hydrogels can be distinguished:

- Homopolymeric: formed from a single monomer that is repeated.
- Copolymeric: formed from two or more monomers with at least one hydrophilic component. Said component can be found joined randomly, in a block or following an alternating configuration.
- Multipolymer Interpenetrating polymeric network (IPN): they are made up of two independent polymers (synthetic or natural), cross-linked to form the polymeric network.

1.1.5.2 Classification based on configuration

They depend on their physical structure and chemical composition, and can be divided into:

- Amorphous (non-crystalline)
- Semicrystalline: combination of amorphous and crystalline phases
- Crystalline

1.1.5.3 Classification based on type of cross-linking

Depending on the nature of cross-linking, they can be divided into chemical or physical cross-linking:

- Chemically cross-linked networks: they are formed by chemical bonds, permanent unions.
- Physically cross-linked networks: formed by non-permanent bonds such as ionic interactions, hydrogen bonds or hydrophobic interactions.

1.1.5.4 Classification based on physical appearance

Depending on their physical appearance, hydrogels are found as matrix, films or microspheres. This appearance depends on the polymerization technique used for the synthesis of the polymer.

1.1.5.5 Classification based on network electrical charge

Finally, according to the absence or presence of localized electrical charge in the cross-linked polymeric chains, four types can be distinguished:

- Non-ionic (neutral)
- Ionic (anionic or cationic)
- Amphoteric electrolytes: containing acidic and basic groups
- Zwitterionic: containing anionic and cationic groups in each repeating unit

1.1.6 Preparation methods

The hydrogels commonly used in drug delivery are generally formed outside the body and the drug is encapsulated in them before introducing the hydrogel-drug system into the body [1].

Depending on the type of crosslinking, it has already been seen that they are divided between physical and chemical:

- Physically cross-linked hydrogels

  A physical cross-linking between the polymer chains of a gel is achieved from a wide variety of physical-chemical interactions such as hydrophobic, ionic or electrostatic interactions, crystallization, hydrogen bonds, or a combination of the above [1].

  These interactions do not require chemical modification or the use of cross-linking agents or initiators, which leads to weak physical bonds.

- Chemically cross-linked hydrogels

  Contrary to what happens with physical cross-linking, in this case there is a chemical reaction, generally formed by the monomer, the initiator and the cross-linker. This reaction gives rise to the formation of covalent bonds that give hydrogels good mechanical strength [1].

The most important polymerization techniques are described below [19]:

1.1.6.1 Bulk polymerization

Bulk hydrogels can be obtained with one or more monomers. To carry out this polymerization technique, a small amount of cross-linker is added to any possible hydrogel formulation and the reaction is initiated either with radiation, or chemical or ultraviolet catalysts.

Thanks to the bulk polymerization, a high rate and degree of polymerization are achieved, due to the high concentration of monomer [19].

1.1.6.2 Solution polymerization/cross-linking

Initially, the monomers (ionic or neutral), are mixed with the crosslinking agent and the reaction is thermally initiated by ultraviolet irradiation or by a redox initiator system.

In this case, the hydrogels obtained must be washed to remove impurities, including traces of monomers, oligomers or the crosslinking agent.

The reaction is carried out in the presence of a solvent that must also be removed after the formation of the hydrogel [19].

1.1.6.3 Suspension polymerization or inverse-suspension polymerization

It is a dispersion polymerization and it is an advantageous method since the products obtained are in the form of powder or microspheres, so grinding is not necessary.

The term "inverse-suspension" polymerization is used since the process that is carried out is a water-in-oil (W/O) process instead of an oil-in-water (O/W) process, which is the one commonly used.

This technique consists of dispersing the monomers and the initiator in the hydrocarbon phase, getting a homogeneous mixture. The drawback is that said dispersion is thermodynamically unstable and requires continuous stirring and the addition of a low hydrophilic-lipophilic-balance (HLB) suspending agent [19].

1.1.6.4 Grafting to a support

This technique is used to improve the mechanical properties of hydrogels prepared with bulk polymerization techniques. It consists of generating free radicals on a stronger support surface and polymerizing the monomers directly on it, forming covalent bonds between the monomers and the support [19].

1.1.6.5 Polymerization by irradiation

Irradiation polymerization consists in irradiating the aqueous polymer solution with gamma rays as initiator, resulting in the formation of free radicals in the polymer chains. These radicals recombine forming covalent bonds between macro-radical chains.

This method has a very important advantage since, thanks to radiation as a reaction initiator; the final polymer obtained is purer and free of chemical initiators [19].

1.1.7 Hydroxypropyl methylcellulose hydrogel

Many hydrogel systems use covalent bonds for their formation. These types of links are what contribute to the system having a strong, elastic and robust polymeric structure; the problem is that these materials may suffer limitations due to their irreversibility [20].

For this reason, moldable hydrogels that can be formed before use and subsequently applied have been developed and investigated as an alternative to covalently linked hydrogels in pharmaceutical applications such as drug delivery, gap filling or tissue engineering, among others [20].

One of the most important requirements is the injectability of the hydrogel in the body in biomedical applications, since the hydrogel must be easy to apply with the use of needles [20, 21, 22]. To ensure this condition, hydrogels must have a viscous flow under shear stress, called shear-thinning; and rapid recovery when the stress ceases, known as self-healing [20].

The shear-thinning behaviour allows obtaining a pre-formed gel with the required physical characteristics, synthesized ex vivo, which is then released in vivo by the application of shear stress during injection through a syringe needle [21].

In addition, the recovery of the elastic modulus after shearing (self-healing) will be faster in shear-thinning hydrogels than in a gelation process of other types of hydrogels.

Self-assembly of functional materials due to non-covalent intermolecular interactions provides moldable, reversible and therefore injectable hydrogels with shear-thinning and self-healing properties [20, 21].

One of the most recently studied hydrogels of this type is the one that appears in the study by Appel et al. [22] in which an injectable shear-thinning supramolecular polymer-nanoparticle (PNP) hydrogel is synthesized, made from a mixture of dodecyl-modified hydroxypropylmethylcellulose ($HPMC_{12}$) and core-shell nanoparticles.

HPMC was chosen for this study as the main polymer due to its high solubility, molecular weight, functionality and biocompatibility [20]. On the other hand, the nanoparticles used were obtained from a copolymer based on polylactic acid (PEG-b-PLA), which allowed them to be encapsulated as hydrophilic molecules in the bulk of the hydrogel, and also allowed to load the nanoparticles with hydrophobic molecules [20, 22].

This completely biocompatible system was tested in vivo in immunocompetent mice [22]. In the immunocompetent mice, the PNP hydrogel significantly increased cell retention over the course of two weeks. PNP hydrogels in combination with therapeutic cells can be used to direct the fate of surrounding cells and tissues to increase the efficacy of clinical treatments [22].

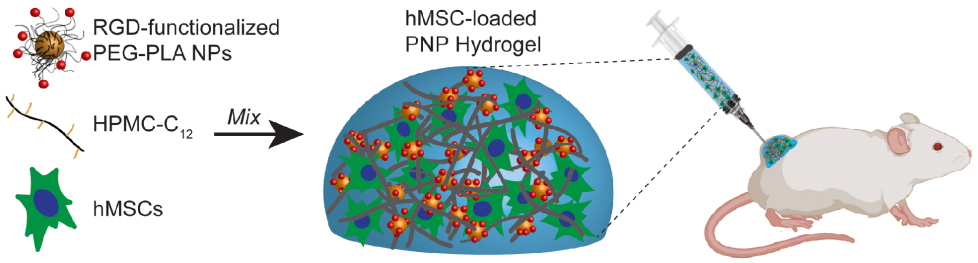

Figure 7: Loading process and injection of the PNP hydrogel in vivo in immunocompetent mice [22]

1.1.8 Agar–carbomer based hydrogels

Agar-carbomer hydrogels, briefly named with the AC_x acronym is synthesized from the two monomers which give its name: Agarose and Carbomer 974P by a statistical block polycondensation [23].

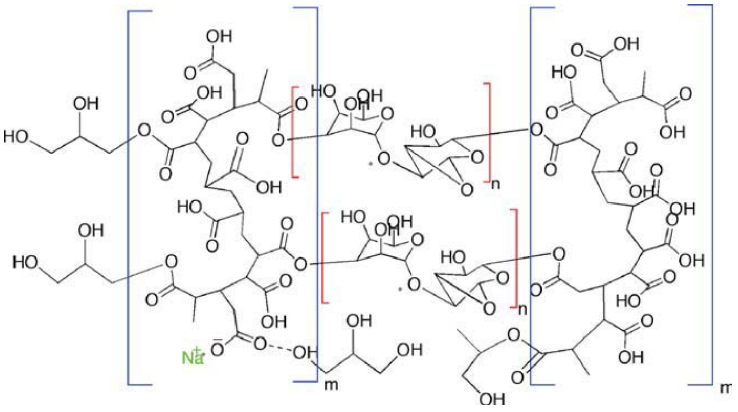

Figure 8: Scheme of the ·D network formed by statistical polycondensation between Agarose (red), Carbomer 974P (blue) and cross-linking agents (green) [24]

Agarose is a commonly used natural polysaccharide, while Carbomer 974P is a highly branched synthetic polyacrylic acid [24]. Said mixture of polymers can be adjusted using different proportions of cross-linking agents to obtain different materials (AC_x) useful for different uses within the field of drug delivery [23].

The importance of this hydrogel is its high biocompatibility and its pH-responsive capacity, which makes it especially useful when simulating living tissue in tissue engineering.

In a study by Rossi et al. [23], the degradation behaviour of agar-carbomer based hydrogels for drug delivery applications was analyzed. In this study it was confirmed that AC hydrogels are pretty anionic and it is this electrostatic nature, confirmed by mass equilibrium swelling at different pH, what influences the ability and kinetics involved in drugs release.

In the precedent thesis to this one, drug release was performed from a polymer-nanoparticles system with agar-carbomer hydrogel [39].

To verify the release efficiency of the organic nanoparticles used, release tests were carried out with pyrene as drug simulator. The amount of pyrene released in an acidic aqueous medium (pH 5) at different temperatures was subsequently analyzed by UV spectroscopy.

From the results obtained, a representation of the cumulated percentage of drug released from the loaded nanoparticles in the agar-carbomer hydrogel was generated.

What was observed was that the amount of drug released at 37 ºC began to grow slowly up to 96 hours and then stabilized, releasing only 14% of the initially loaded pyrene. On the other hand, in the tests carried out at 42 ºC, the release percentage was much higher, reaching 40% in the first hours and reaching a 60% release of the initially loaded pyrene (Figure 9).

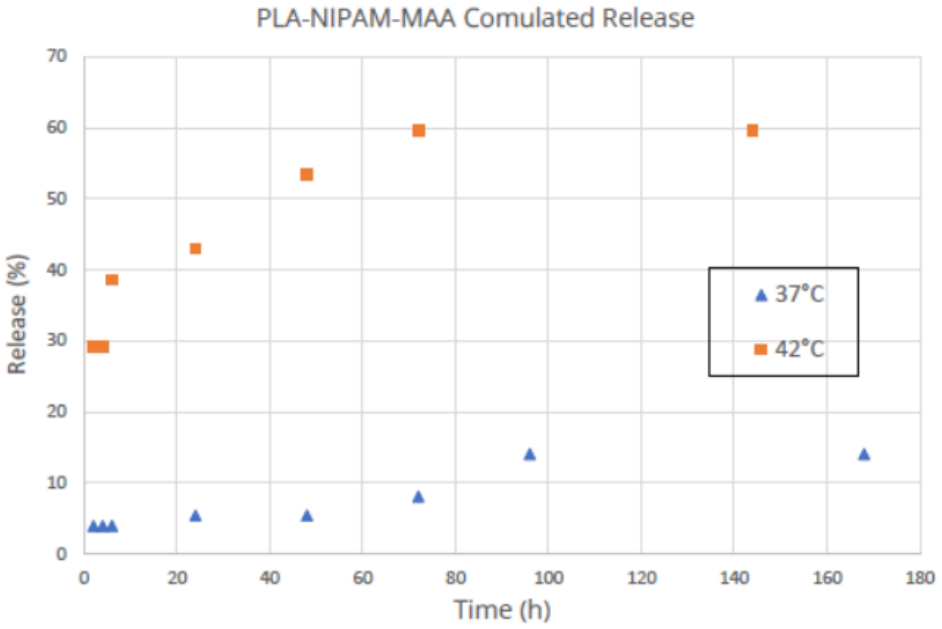

Figure 9. Cumulated release of pyrene in a polymer-nanoparticles system with agar-carbomer hydrogel

1.2 Nanoparticles based on polyNIPAm

Currently, nanotechnology focuses on the research and development of therapeutic nanoparticles combined with other materials to form hybrid systems for biomedical applications. These nanoparticles are known as smart nanoparticles due to their core-shell structure and properties [25, 26].

Smart nanoparticles can be introduced into the hydrogel network in two ways: by mixing directly with a monomer solution followed by gelation; or they can be incorporated into the hydrogel matrix after its formation, being trapped by the gel after its swelling [25].

The need to find a more controlled form of drug release has led the scientific community to study different types of nanoparticles that respond to changes in pH and temperature, with the aim of achieving a more localized drug release. These nanoparticles change their structure and thus release the drug depending on the pH and temperature on the surrounding environment.

Among many other biomedical applications, the use of smart nanoparticles in cancer treatments stands out. Cancer cells have a lower pH than that of the extracellular fluid, so that the nanoparticles can vary their pH when they come into contact with said cells from 7,4 to 5 via cellular proton effect, also known as endocytosis process [26].

1.2.1 PNIPAm features

Poly(N-isopropylacrylamide) (PNIPAm) is one of the most studied biocompatible polymers. It is a water-soluble and hydrophilic polymer, which presents an extended chain conformation below 32 ºC, its LCST [26, 27].

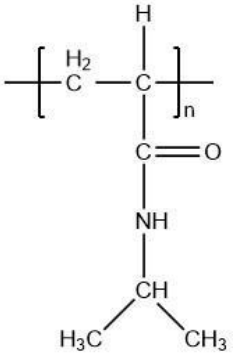

Figure 10: PNIPAm structure

When its LCST is exceeded, PNIPAm undergoes a coil-globule phase transition, which leads to a change in its structure, becoming a hydrophobic polymer [27]. This transition occurs in a narrow temperature range and is reversible [28].

It is for this reason and for its ability to adopt different shapes and morphologies that PNIPAm has become one of the most interesting polymers in the biomedical field for on-off drug release and attachment/detachment of cultured cells [28].

1.2.2 PNIPAm based copolymers

PNIPAm-based copolymers combined with hydrophobic segments are able to form micellar core-shell structures below the LCST of PNIPAm (32 ºC) [30]. This combination creates a hydrophilic shell formed by the hydrated PNIPAm and a hydrophobic interior with the added groups [28].

In addition, the interior of the formed nanoparticles can be loaded with hydrophobic drugs, while the outer shell gives them stability in water and thermo-responsive properties [28].

The correct selection of the segments that will form the copolymers by block copolymerization is important, since they will be responsible for delivering the drug directed to the tumor area.

Polymeric micelles with a hydrophilic PNIPAm outer shell and a favorable size of less than 100 nm are able to present specific targeting of solid tumor sites by a passive-type mechanism. The thermo-responsive ability of these micelles may be able to increase targeting efficiency through a stimuli-responsive targeting process that uses local heating in tumor areas [28].

The use of these polymeric micelles that respond to changes in temperature can achieve a temporary control of drug release, since the drug expresses its bioactivity only for a period of time defined by local heating and cooling [28].

1.2.3 Biomedical applications and biocompatibility of PNIPAm based copolymers

The use of PNIPAm-based copolymers in biomedical applications is widespread. This thesis focuses on PNIPAm-based nanoparticles for the controlled release of drugs, but there are also other fields in which they can be very useful, such as 3D-scaffold platforms for tissue engineering, carriers for cell encapsulation, and adhesive or barriers between tissue and material surfaces, among others [29].

Biocompatibility is defined as "the ability of a material to perform with an appropriate host response in a specific application", and it is essential that the material does not induce toxicity and allows good cell proliferation and distribution [27].

There are numerous studies that prove the biocompatibility of PNIPAm-based polymers. For example, in the field of tissue engineering, it has been shown that cells taken from patients can be cultivated in PNIPAm or other substrates covered with PNIPAm, forming viable cell sheets that can eventually form a tissue. The absence of cytotoxicity in a large number of cells adhered to PNIPAm surfaces together with high rates of cell proliferation has also been confirmed. When the cells adhere to said surface, it means that the material that makes up the surface is bioadhesive and biocompatible [27].

1.2.4 Core-shell nanoparticles based on poly(D,L-lactide)-g-poly(N-isopropylacrylamide-co-methacrylic acid)

Core-shell nanoparticles can self-assemble from amphiphilic block copolymers or amphiphilic graft copolymers by hydrophobic segment self-aggregation and hydrophilic segment contacting with the water phase [26].

In this thesis work, the synthesized nanoparticles were of poly(D, L-lactide)-g-poly(N-isopropylacrylamide-co-methacrylic acid), obtained by grafting poly(D,L-lactide) (PLA) onto the hydrophilic backbond of poly(N-isopropylacrylamide-co-methacrylic acid) (p(NIPAm-coMAA)), forming core-shell nanoparticles with environmental sensitivity and biodegradability following the experimental study by Lo et al. [26].

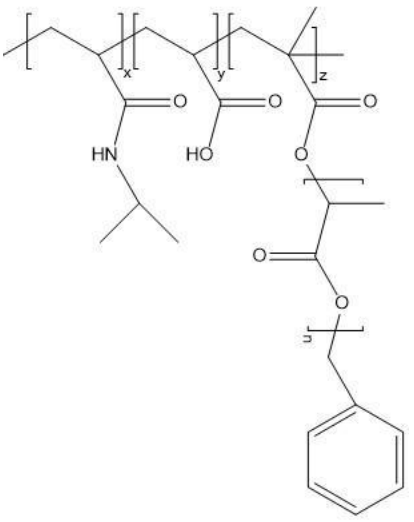

Figure 11: PLA-P(NIPAm-co-MAA) graft copolymer structure

PNIPAm is among the group of polymers that have a lower critical temperature of solubility, collapsing at 32 ºC. It has the sharpest swelling transition within the thermosensitive alkyl acrylamide polymers [30].

In contrast, methacrylic acid (MAA) polymers are known for their sensitivity to changes in pH. They are capable of swelling up to 10 times their dry weight in basic solutions and collapsing in acid solutions due to electrostatic repulsion between the carboxylic acid side chain and the ions present in the solution [30].

What is achieved by introducing a small proportion of MAA in PNIPAm polymers is to raise the LCST of the copolymer above 37 ºC, due to the hydrophilic effect of said incorporation and, in addition, turning it into a copolymer sensitive to changes in pH [26]. Increasing the amount of MAA increases the LCST as the polymer becomes more hydrophilic thus causing more ionic repulsion. In addition, the effect of the PLA segment results on the formation of a core-shell nanoparticle environmentally sensitive and biodegradable.

Thanks to their ability to deliver small amounts of drug to the desired area, environmentally sensitive polymers can encapsulate hydrophobic drugs and can be used to increase the effectiveness of therapies by achieving a more localized drug release.

1.2.4.1 Synthesis

The synthesis of PLA-P(NIPAm-co-MAA) graft copolymer is formed by three consecutive reactions, according to the study carried out by Lo et al. [26]:

- Synthesis of PLA:

  Polylactic acid is first synthesized by a ring-opening cationic polymerization of D,L-lactide. This reaction is initiated by benzyl alcohol and catalyzed by stannous octoate ($Sn(Oct)_2$), using toluene as solvent.

- Synthesis of PLA-MA:

  The second step is the polylactic acid methacrylation reaction. This reaction consists on an esterification of the terminal hydroxyl group of PLA using methacryloyl chloride (MACl) and using anhydrous toluene as solvent.

- Synthesis of PLA-P(NIPAm-co-MAA) graft copolymer:

  Finally, the graft copolymer PLA-P(NIPAm-co-MAA) is obtained by a free radical polymerization mechanism. To do it, PLA-MA, MAA and NIPAm are used using acetone as a solvent.

  The nanoparticles are obtained by performing a dialysis and a subsequent lyophilization.

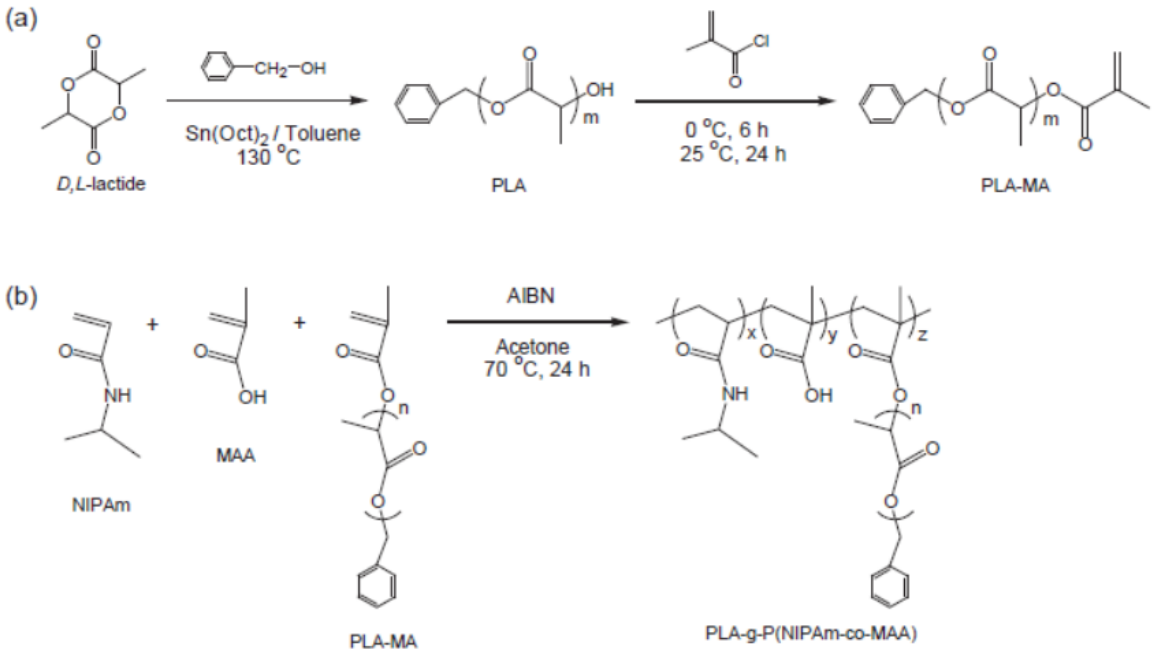

Figure 12: Reaction scheme for (a) PLA-MA macromonomer and (b) PLA-P(NIPAm-co-MAA) graft copolymer [26]

1.2.4.2 Drug release

In the study carried out by Lo et al. [26], the behaviour of the release of nanoparticles loaded with pyrene as drug simulator at pH 5 and pH 7.4 and 37 ºC was analyzed. It shows that drug release from nanoparticles in an aqueous environment is strongly controlled by the pH of the solution.

It was observed that in the acidic environment the discharge percentage was high: from 25% in the first hour to 80% in four days. In contrast, in the neutral environment, the discharge was lower, not reaching the 20% [Fig. 12].

In conclusion, this system allows controlled drug release over time. These results suggest that drug release is controlled by the collapse of the nanoparticle's outer shell due to structural deformation.

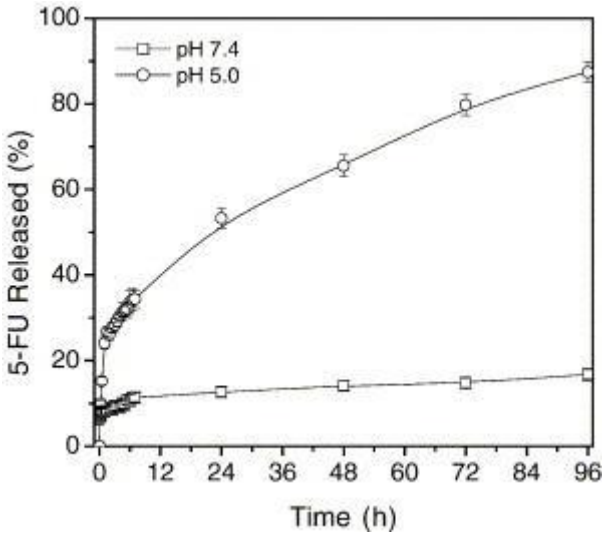

Figure 13: Pyrene release by PLA-g-P(NIPAm-co-MAA) nanoparticles at 37 °C in different pH conditions [26]

1.3 Hybrid hydrogel systems

1.3.1 Nanoparticles-hydrogel systems

With the aim of improving the localized application of medical therapies, the combination of nanoparticles with hydrogels has gained popularity due to the fact that it provides a biocompatible hybrid material for controlled drug release [25].

The nanoparticles can be encapsulated in the hydrogel network either by mixing with the solution and then gelling, or they can be incorporated into the hydrogel matrix after formation. This last case is especially useful in cases where nanoparticles can interfere with gel formation [25].

Hybrid nanoparticle-hydrogel systems, also called NP-gels, manage to integrate two different materials in the same formulation with physical, chemical and biological properties that neither could achieve separately.

These systems consist of the encapsulation of molecules in nanoparticles, which are then encapsulated in the hydrogel matrix. These systems can be synthesized and subsequently administered orally, nasally, or injected into patients in a minimally invasive manner [45].

1.3.2 Mathematical approaches

In a study by Lin et al. [45], two mathematical approaches were used to predict drug release from the nanoparticles encapsulated in the hydrogel:

- Macroscopic diffusion models:

  In macroscopic modeling, the most applicable models are those based on Fick's second law of diffusion. In such models, the size and geometry of the particle, as well as the surface area, are the most important parameters.

  The accuracy of any diffusion model in predicting drug release from the system depends on the accuracy of the estimated diffusivity.

- Microscopic Monte Carlo simulations:

  This method has been successfully proved to describe the transport behavior of molecules within biodegradable systems and has also been applied to networks of hydrophobic polymers such as PLGA [45].

  Unfortunately, the accuracy of these models is highly protein specific.

1.3.3 Applications of NP-gels

Three main areas in the field of application of NP-gels were studied by Gao et al. [25].

1.3.3.1 Passively controlled drug release

Drug molecules encapsulated in the hydrogel network are released by diffusion, swelling, and chemically controlled mechanisms. At the same time, nanoparticles control release kinetics through their tailored structure, particle size, and manufacturing conditions. By integrating the two platforms, NP-gels create hierarchical matrices with remarkable versatility in modulating drug release kinetics for various delivery purposes, which is difficult for either platform to achieve alone. Hydrogels can exhibit tissue-like properties but suffer from erratic release and rapid diffusion of drug molecules from the polymer matrix. In contrast, NP gels that use nanoparticles as drug depots can overcome this drawback and significantly extend the duration of drug release.

In addition to single drug delivery, NP-gels also combine rapid diffusion-driven release of drug molecules dispersed directly in the hydrogel network with slow release of drugs from nanoparticle reservoirs [25].

1.3.3.2 Stimuli-responsive drug delivery

Intelligent hydrogels that dramatically change their volume in response to environmental stimuli such as temperature, pH, and chemical signals are attractive biomaterials for drug delivery. This responsiveness can be coupled with additional

signals such as light and magnetic field via nanoparticles embedded in the matrix, creating unique NP gels that can remotely control drug release.

The use of nanoparticles as the only building blocks to form a cohesive gel-like network represents a new class of NP-gels. The combination of oppositely charged nanoparticles, particularly those already established as nanocarriers for pharmaceuticals, is a common approach for preparing this type of NP-gel. For example, positively charged dextran nanoparticles coated with chitosan and negatively charged dextran nanoparticles coated with alginate were mixed to form a colloidal hydrogel for glucose-dependent and self-regulated insulin delivery (Figure 14). At the macroscopic level, the construct was made with nanoparticles that provided sufficient cohesive force for gelation. This cohesive force decreased at high shear rates, resulting in low viscosities suitable for injection. At the microscopic level, the nanoparticles allowed simultaneous delivery of insulin and two glucose-responsive enzymes. In a hyperglycemic state, glucose was catalytically converted to gluconic acid, leading to dissociation of the gel-like network and subsequent release of insulin.

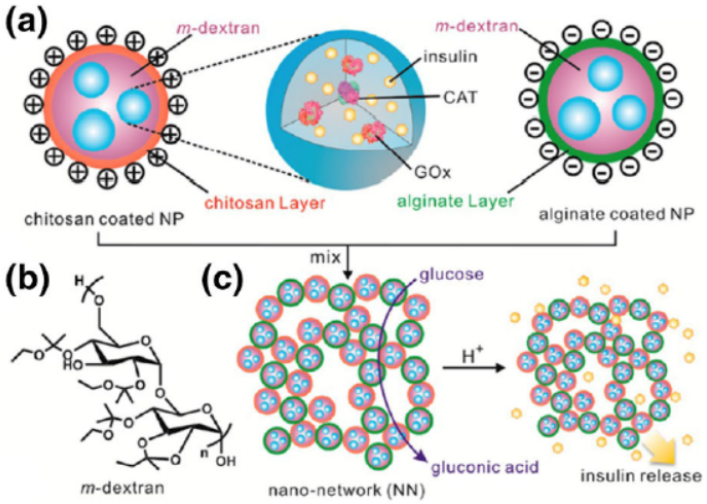

Figure 14. Insulin release process from chitosan and alginate coated NPs [25]

An alternative approach to colloidal gel formation is the use of nanoparticles with sensitive hydrophobic interactions. In this approach, the nanoparticles typically consist of a core of a hydrophobic polymer and a shell of a thermoreactive polymer that undergoes a transition from hydrophilic to hydrophobic in response to a

change in temperature. If the temperature is below a critical temperature, the polymer shell is water soluble and stabilizes the nanoparticles. However, if the temperature is above a critical temperature, the polymer shell becomes hydrophobic, causing the dispersed nanoparticles to flocculate into a hydrogel network [25].

1.3.3.3 Site-specific drug delivery

NP-gels trap nanoparticles in 3D polymer matrices for better local drug delivery. Various NP-gel formulations have been developed to target drugs to disease sites in the spinal cord, eye, and skin. In these formulations, drug localization depends primarily on the properties of the hydrogel network, allowing nanoparticle design to focus exclusively on modulating drug release [25].

Site-specific targeting of drugs can also be achieved by modifying hydrogels with targeting ligands that are able to bind specifically to disease sites. For example, a silver-releasing antibacterial NP-gel consisting on silver nanoparticles and tissue-adhesive hydrogel has been developed by Gao et al. [25].

1.3.4 Examples of NP-gel systems and its applications

Nowadays there are numerous studies that prove the proper functioning of NP-gel systems in the biomedical field and that they are successfully used in different applications.

1.3.4.1 RGD-functionalized PEG-PLA NPs and HPMC-C_{12} hydrogel

In a study carried out by Grosskopf et al. [22], NP-gel systems for stem cell delivery to native tissue aids in tissue regeneration were synthesized and tested. Hydrogels can increase local cell retention and engraftment at the injection site compared to traditional liquid injections.

The nanoparticles used in this study were made of poly(ethylene glycol)-poly(lactic acid) functionalized with arginine-glycine-aspartic acid (RGD-functionalized PEG-PLA). PEG-PLA was functionalized with RGD to promote cell adhesion and viability.

The hydrogel used was functionalized with 1-dodecyl isocyanate hydroxypropyl methylcellulose (HPMC-C_{12}).

The NPs were loaded with human mesenchymal stem cells (hMSCs).

Furthermore, it was shown that the system exhibiting a yield stress can prevent cell setting across translationally relevant time-scales and aid in integration with native tissue.

1.3.4.2 PEG-b-PLA NPs and HPMC-C_{12} hydrogel

Apple et al. [20] carried out a study in which they synthesized two types of nanoparticles that were subsequently encapsulated in an HPMC hydrogel for drug delivery.

In the first system studied, the nanoparticles used were poly(ethylene glycol)-b-poly(lactic acid) (PEG-b-PLA) as a vehicle for drug release in in vivo applications. The hydrogel used was functionalized hydroxypropyl methylcellulose (HPMC-C_{12}).

The use of the functionalized HPMC was due to the fact that the presence of PEG in the nanoparticles reduced the mechanical properties and the affinity with the non-functionalized HPMC.

Fluorescein isothiocyanate-labelled bovine serum albumin (BSA-FITC) and Oil Red (OR) were used as drug simulants in the release tests, obtaining a greater amount of drug released with BSA-FITC than with OR.

1.3.4.3 Carboxy-functionalized PS NPs and HPMC-C_{12} hydrogel

This was the second system studied by Appel et al. [20].

The nanoparticles used were carboxy-functionalized polystyrene (PS), encapsulated in a functionalized hydroxypropyl methylcellulose hydrogel (HPMC-C_{12}).

Said system presented good interactions between the hydrophobic chains of the hydrogel and the hydrophobic core of the nanoparticles. Furthermore, this system had an elastic modulus three times stronger than previously studied systems with non-functionalized HPMC, indicating an increase in the interaction energy between the hydrogel and the NPs.

Fluorescein isothiocyanate-labelled bovine serum albumin (BSA-FITC) was used as a drug simulant in the release tests.

1.3.4.4 PAMAM NPs and PEGD-MA hydrogel

In a study carried out by Wang et al. [46], a NP-gel system was synthesized and used for platensimycin (PTM) delivery in skin infections caused by methicillin-resistant Staphylococcus aureus (MRSA).

To facilitate the use of PTM against MRSA infections, they prepared polyacrylamide hydrogels, formulated with acrylamide and poly(ethylene glycol) dimethacrylate (PEGD-MA), in which polyamidoamine (PAMAM) nanoparticles were inserted. The PAMAM nanoparticles were loaded with PTM.

In a MRSA-infected skin model, this NP-gel system exhibited excellent antibacterial activity and such rapid wound healing effects. The NP-gel(PTM) formulation significantly reduced the number of MRSA colonies and accelerated the healing of wounds.

1.3.4.5 Polyion complex NPs and alginate solution hydrogel

Lim et al. [47] performed a study in which they synthesized a nanoparticles-hydrogel system in order to induce the chondrogenesis of mesenchymal stem cells (MSCs) for cartilage tissue engineering.

Polyion complex (containing TGF-β_2, which is a transforming growth factor-beta included in MSCs) was used for the nanoparticles and a gelation rate controllable alginate solution (containing BMP-7, a bone morphogenic protein) as hydrogel.

This system showed a controlled release of both growth factors: a faster release of BMP-7 and a slower release of TGF- β_2, which provide highly desirable delivery kinetics for cartilage regeneration, as well as chondrogenesis of MSCs.

2. Materials and methods

2.1 Nanoparticles based on poly(D,L-lactide)-g-poly(N-isopropyl acrylamide-co-methacrylic acid)

For the synthesis of poly(D,L-lactide)-g-poly(N-isopropyl acrylamide-co-methacrylic acid), three consecutive reactions previously defined by Lo et al. [26] were performed.

2.1.1 Materials

- D, L-Lactide (Sigma Aldrich)
- Benzyl alcohol (Sigma Aldrich)
- Stannous octoate ($Sn(Oct)_2$, Sigma Aldrich)
- Toluene (Sigma Aldrich)
- Triethylamine (TEA, Sigma Aldrich)
- Methacryloyl chloride (MACl, Sigma Aldrich)
- Methacrylic acid (MA, Sigma Aldrich)
- N-Isopropylacrylamide (NIPAm, Sigma Aldrich)
- 2,2'-Azobis(2-,methylpropionitrile) (AIBN, Sigma Aldrich)
- Acetone (Sigma Aldrich)
- Diethyl ether (Sigma Aldrich)
- Dichloromethane (DCM, Sigma Aldrich)
- Hexane (Sigma Aldrich)
- Dimethyl sulfoxide (DMSO, Sigma Aldrich)

2.1.2 Synthesis of polylactic acid (PLA) from D, L-Lactide by ring opening polymerization

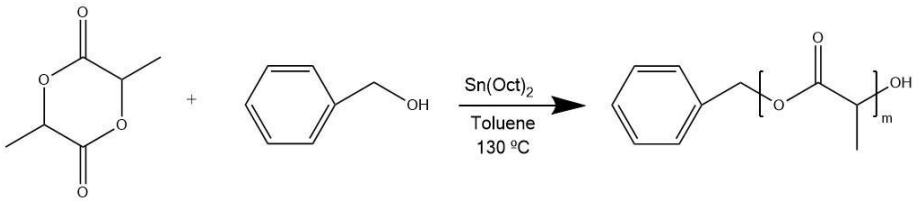

Figure 15. Reaction scheme for the synthesis of PLA

Table 1. Detailed recipe for the synthesis of PLA

COMPOUND	MW [g/mol]	g	mmol	eq	mL
D,L-Lactide	144,13	3,22	22,34	13	-
Benzyl alcohol	108,14	0,18	1,72	1	0,0172
$Sn(Oct)_2$	405,12	0,0035	0,0086	0,005	-
Toluene	92,14	34,8	377,68	228,3	40

To prepare the reaction, a two-neck flask was used, and 3,22 g of D,L-Lactide were placed on it.

Then, 40 mL of toluene were added under a continuous flow of nitrogen and the mixture was stirred in an oil bath at 130 ºC.

Afterwards, 0,0035 g of stannous octoate were added with 0,172 mL of benzyl alcohol and the mixture went under stirring and under nitrogen for 4 hours at 130 ºC.

- Purification

  For the purification step, 50 mL of diethyl ether were placed in an Erlenmeyer flask and put in freezer for 30 minutes; afterwards, the reaction product was dropped into the Erlenmeyer containing the diethyl ether. The flask was left in freezer until the precipitate was formed. Then, the liquid was recovered using a pipette and dried in the rotavapor under vacuum.

2.1.3 Synthesis of Polylactic Acid Methacrylate (PLA-MA)

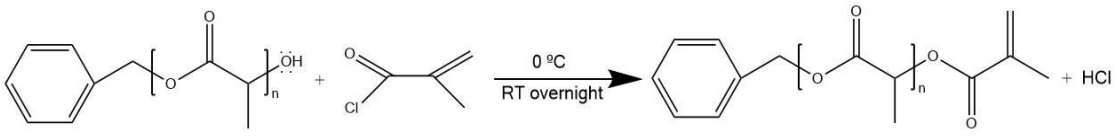

Figure 16. Reaction scheme for the synthesis of PLA-MA

Table 2. Detailed recipe for the synthesis of PLA-MA

COMPOUND	MW [g/mol]	g	mmol	eq	mL
PLA	987	1,09	1,1	1	-
Triethylamine	101,19	0,33	3,27	2,97	0,454
Methacryloyl chloride	104,53	0,28	2,725	2,47	0,261
Anhydrous toluene	92,14	-	-	-	50

To prepare the reaction, it was first necessary to anhydrify the toluene, which was the solvent used to carry out the reaction. To do this, approximately 70 mL of toluene were placed in a flask and sodium sulfate was added. It was then filtered and collected in another dry flask.

1,09 g of PLA were transferred to a 3-neck balloon flask and dried on the rotary evaporator.

Anhydrous toluene was then added to the balloon flask on ice, at 0°C and under a continuous flow of nitrogen.

TEA and methacryloyl chloride were also added, always under nitrogen flow.

After all reagents were added, the reaction was left running overnight at room temperature under nitrogen atmosphere.

- Purification

  In this case, the purification stage consists of two steps: first an extraction with dichloromethane and water and, later, a precipitation with dichloromethane and hexane.

  - Extraction

    The extraction was performed with dichloromethane and distilled water. To carry it out, a separator was used where the methacrylation reaction product, 10 mL of dichloromethane and 10-15 mL of distilled water were added. Due to the density, the dichloromethane remains at the bottom of the separator. Both parts were separated: organic phase and aqueous phase. The organic phase was dried under vacuum.

Figure 17: Purification of PLA-MA by extraction with DCM and distilled water

- Precipitation

  Once the separation was done, it was necessary to remove the methacryloyl chloride from the organic phase. To do so, the dry organic phase was dissolved in 3 mL of dichloromethane. Afterwards, in a balloon flask with 100 mL of hexane, previously placed in the freezer, the organic phase was dropped; the flask was then put back in the freezer and waited for it to precipitate.

  The precipitate was then dried on the rotary evaporator.

2.1.4 Synthesis of PLA-g-P(NIPAm-co-MAA) graft copolymer

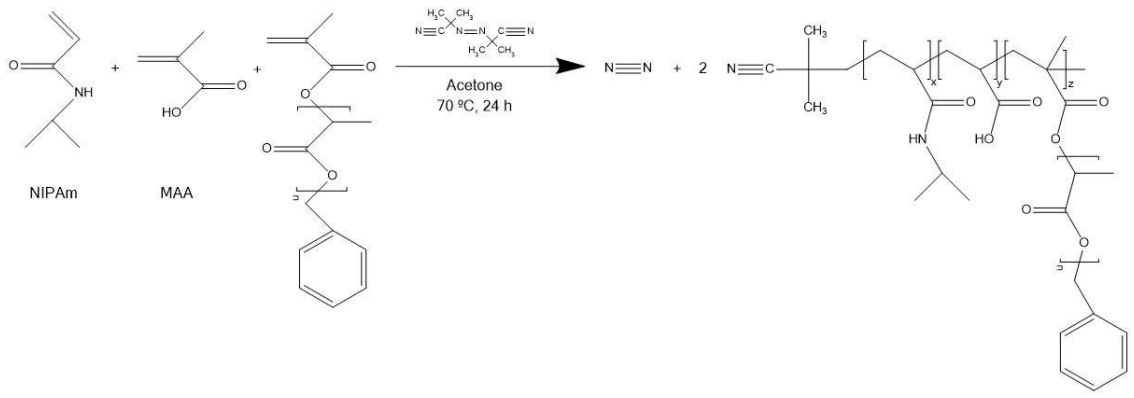

Figure 18. Reaction scheme for the synthesis of PLA-g-P(NIPAm-co-MAA)

Table 3. Detailed recipe for the synthesis of PLA-g-P(NIPAm-co-MAA)

COMPOUND	MW [g/mol]	mg	mmol	eq	mL
PLA-MA	1192	90,54	0,09	3,3	-
Methacrylic Acid	86,09	20,22	0,27	8,7	0,0199
NIPAm	113,16	268,86	2,376	88	-
AIBN	164,21	4,47	0,027	1	-
Acetone	58,08	-	-	-	26,3

To carry out the copolymerization reaction, PLA-MA was dissolved in a small amount of dichloromethane, calculating the concentration and the volume that should be taken to obtain the 90,54 mg necessary for the reaction. The necessary mL were taken and dried in a rotary evaporator in a three-necked balloon flask.

Once dried, 5,3 mL of acetone, the methacrylic acid and the NIPAm were added to the flask, under a continuous flow of nitrogen and a temperature of 70 ºC.

Then 4,47 mg of AIBN, which was the initiator of the reaction, were dissolved in 1 mL of acetone. The solution was added to the flask with a syringe, always under a continuous flow of nitrogen.

Four hours later other 20 mL of acetone were added and the reaction went for 24 hours at 70°C and under nitrogen.

- Purification

  The purification step in this case consists on a precipitation.

  First, a 250 mL balloon flask was filled with 150 mL of diethyl ether and placed in the freezer for 30 minutes. After that, the copolymerization product was added dropwise into the diethyl ether flask with a Pasteur pipette and allowed to cool and precipitate in the freezer again for about 20 minutes.

  Once it had precipitated, the diethyl ether was extracted.

  Finally, the precipitate was dried in a rotary evaporator.

Figure 19: Result of precipitation step

2.1.5 Organic nanoparticles preparation

To obtain the nanoparticles, a dialysis was prepared. To do it, the already purified copolymerization product (PLA-g-P(NIPAm-co-MAA)) was dissolved in 25 mL of dimethyl sulfoxide (DMSO).

The membrane used was a cellulose membrane with a molecular weight cut-off of 14000 Da. To prepare it, the membrane was soaked in distilled water and filled with the DMSO solution, closed and immersed in a distilled water bath with stirring for 48 hours.

Once the 48 hours have elapsed, the solution obtained was frozen and lyophilized to obtain the nanoparticles.

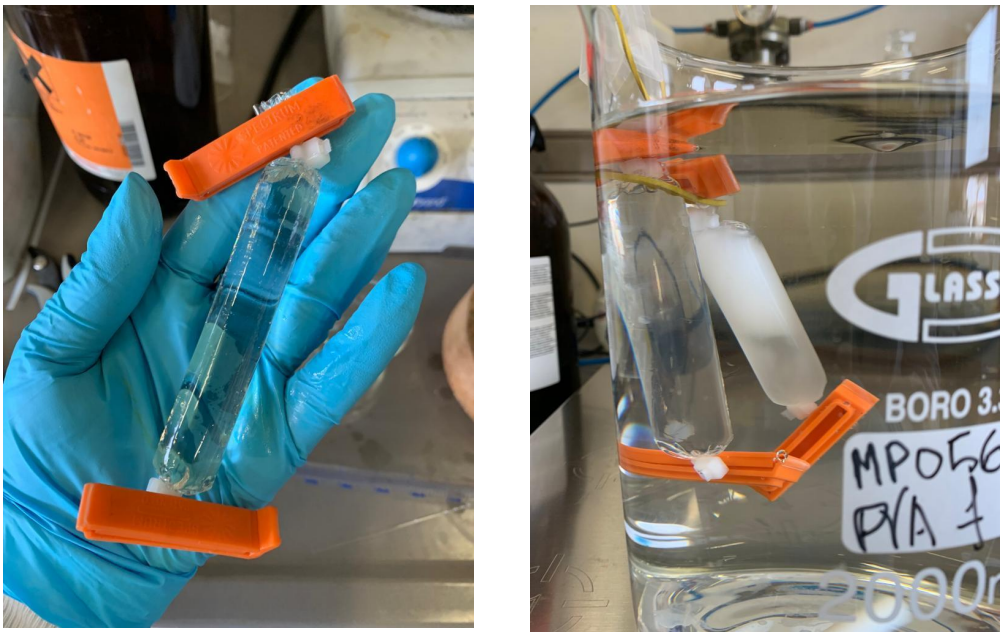

Figure 20: Dialysis before and after NPs formation

2.2 HPMC-C_{12} hydrogels

The reaction for the HPMC functionalization was performed following a previous study from Grosskopf et al. [22].

2.2.1 Materials

- Hydroxypropyl methyl cellulose (HMPC, Sigma Aldrich)
- 1-dodecyl isocyanate (Sigma Aldrich)
- Triethylamine (TEA, Sigma Aldrich)
- N-methyl pyrrolidone (NMP, Sigma Aldrich)
- Acetone (Sigma Aldrich)
- Fluorescein isothiocyanate (FITC, Sigma Aldrich)
- Dimethyl sulfoxide (DMSO, Sigma Aldrich)
- Hydrochloric acid (HCl, Sigma Aldrich)

2.2.2 Hydroxypropyl methyl cellulose (HPMC) functionalization - HPMC-C_{12} synthesis

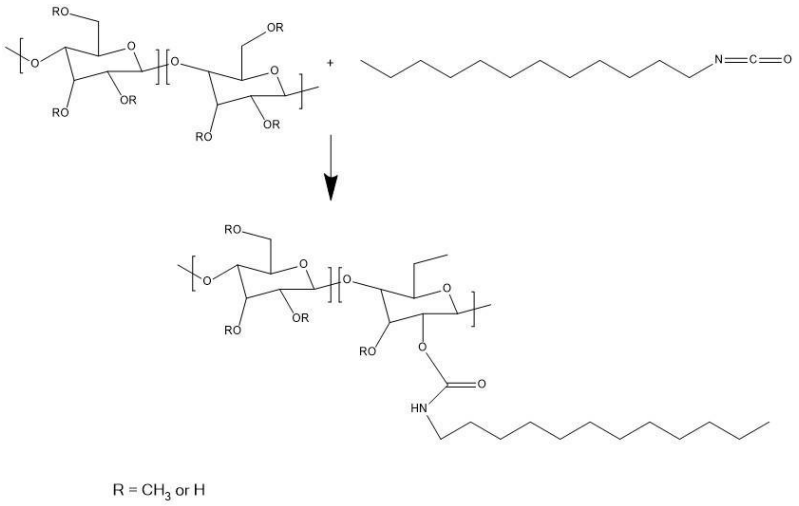

Figure 21: Reaction scheme for the synthesis of HPMC-C_{12}

Table 4: Detailed recipe for the HPMC-C_{12} synthesis

COMPOUND	MW [g/mol]	g	mmol	eq	mL
HPMC	90000	1	0,01	1	-
1-dodecyl isocyanate	211,34	0,105	0,5	50	0,120
Triethylamine	101,19	-	-	-	2 drops
N-methylpyrrolidone	99,13	-	-	-	50

To perform the functionalization of the HPMC-C_{12}, 1 g of HPMC need to be dissolved in 45 mL of N-methylpyrrolidone by stirring at 80 ºC for, approximately, 2 hours.

Once the solution has reached the room temperature, a solution of 0,120 mL of 1-dodecyl isocyanate with 2 drops of TEA was dissolved in 5 mL of NMP. This

solution was then added to the reaction mixture, which was stirred at room temperature overnight.

2.2.2.1 *Purification*

The purification step consists on a precipitation. The solution was dropped into a flask with previously cooled acetone with a Pasteur pipette.

Afterwards, the solution was filtered and the polymer obtained was transferred into a balloon flask and dried in the rotary evaporator.

After the product drying, it was left with distilled water under stirring for a night.

Figure 22: Precipitation of HPMC-C_{12} in cold acetone and filtration

2.2.2.2 *Dialysis*

To prepare the dialysis, the membrane used was a cellulose membrane with a molecular weight cut-off of 14000 Da. To prepare it, the membrane was soaked in distilled water and filled with the HPMC-C_{12} solution, closed and immersed in a distilled water bath with stirring for 24 hours.

Once the 24 hours have elapsed, the solution obtained was frozen and lyophilized.

2.2.3 Drug release from polymer-nanoparticles HPMC based hydrogels

The drug release from polymer-nanoparticles hydrogel consists of three steps: the preparation of the HPMC solution, the solution of nanoparticles, and gel preparation.

- HPMC-C_{12} solution

  After the lyophilization, 240 mg of HPMC-C_{12} were dissolved with 4 mL of distilled water for 48 hours in the shaker to obtain the gel.

  Afterwards, the gel was transferred into a 5 mL syringe. Then, 0,33 g of the gel were transferred from the 5 mL syringe to a 1 mL syringe.

- Nanoparticles solution

  To prepare the nanoparticles solution, 40 mg of nanoparticles were dissolved in 1,566 mL of distilled water.

  After that, 100 μL of a solution of FITC in DMSO with a concentration of 28,8 mg/mL were taken and added to the solution of the nanoparticles. This solution went under stirring for 25 minutes.

  500 μL of this solution were transferred into a 1 mL syringe.

- Gel preparation

  To mix the two solutions, both syringes were joined with a connector and 60 cycles were carried out.

  This process was carried out in three different syringes and three membranes were prepared.

Figure 23: Union system with two syringes and a connector

2.3 Measurements

2.3.1 Nuclear Magnetic Resonance (NMR)

The ^{1}H-NMR experiments were performed using a Bruker AC (400 MHz) spectrometer.

2.3.1.1 Technique

An NMR analysis allows knowing the molecular structure of the sample to be analyzed by measuring the interaction of the nuclear spins when they are placed in a magnetic field [31].

2.3.1.2 Samples preparation for analysis

To prepare the sample for the NMR, a small amount of the sample needs to be dried in the rotary evaporator and dissolved in 0,6 mL of the solvent used for the NMR analysis.

The solvents used were deuterated dimethyl sulphoxide (DMSO-d6), chloroform ($CDCl_3$) and deuterium oxide (D_2O).

2.3.2 Organic Gel Permeation Chromatography (GPC)

The instrument used was a Jasco LC-2000 Plus gel permeation chromatograph equipped with a refractive index detector (RI-2031 Plus, Jasco) using 3 Agilent PLgel columns, 5 × 10^{-6} M particle size, 300×7,5 mm (MW range: 5×10^{12} to 17×10^{5} g mol^{-1}). The GPC samples were injected using a Jasco AS-2055 Plus autosampler. The instrument was calibrated using polystyrene standards.

2.3.2.1 *Technique*

Also known as size exclusion chromatography, it consists on the separation of components depending on their molecular mass or size. The stationary phase is a porous polymeric matrix whose pores are completely filled with the solvent used as the mobile phase. The sample molecules pass through the columns containing this porous gel, so that the molecules that exceed a certain size pass through preferential routes, while those that have a smaller size, pass through the pores exiting later, giving longer retention times [32].

2.3.2.2 *Samples preparation for analysis*

To analyze the samples in the GPC, the product was dissolved in tetrahydrofuran (THF) at the concentration of 4 mg/mL and microfiltered using a 0,2 μm PTFE filter.

2.3.3 UV-vis spectrometry

The spectrometer used was a Tecan® Microplate Reader with UV-vis spectroscopy applying the Lambert-Beer law.

2.3.3.1 *Technique*

UV-vis spectroscopy is a quantitative technique used to determine the concentration of analyte in a given sample solution. To do this, the intensity of light passing through a sample is measured with respect to the intensity of light passing through a reference or blank sample [33]. The presence of analyte in the solution will affect the amount of radiation transmitted through the solution, and, hence, the relative transmittance or absorbance of the solution may be used as an index of analyte concentration [34].

2.3.3.2 *Samples preparation for analysis*

To prepare the samples to be analyzed in the UV, the sample was dissolved in the indicated solvent and, in addition, a cuvette could be prepared with the same solvent used, which would serve as a blank for the analysis.

2.3.4 Dynamic Light Scattering (DLS)

The equipment used was a Malvern Zetasizer Nano ZS at a scattering angle of 173º (backscatter) and polydispersity index (PDI) of the NPs produced.

2.3.4.1 *Technique*

Dynamic Light Scattering is also known as photon correlation spectroscopy or quasi-elastic light scattering.

When a monochromatic light beam meets a solution with macromolecules, the light is scattered in all directions depending on the shape and size of the macromolecules.

It is a technique that mainly measures the Brownian motion of macromolecules in solution, which arises due to the bombardment of solvent molecules, and relates this motion to the size or diffusion coefficient (D_T) of the particles. This movement is influenced by the size, temperature, and viscosity of the solvent [35].

2.3.4.2 *Samples preparation for analysis*

The samples were prepared in a cuvette with a solution of nanoparticles in the same solution at pH 5 used for the releases, and also in a distilled water solution.

2.3.5 Near-infrared Spectroscopy (NIR)

A Varian 640-IR spectrometer equipped with a single bounce ZnSe ATR accessory was used. The attenuated total reflection (ATR) technique was employed, and so the solid powdered samples were directly analysed without treating them with KBr.

2.3.5.1 *Technique*

Its main objective is to analyse a sample to acquire information qualitatively and quantitatively from the interaction of infrared electromagnetic waves with its constituents. This interaction causes alterations in matter that are related to changes in the vibrational state of the molecules. The vibrational spectrum of a molecule is considered a unique physical property and therefore characteristic of each molecule [36, 37].

2.3.5.2 *Samples preparation for analysis*

IR spectroscopy was used to analyse the functionalized HPMC-C_{12}.

This process was done to test both HPMC and HPMC-C_{12} for comparison.

2.3.6 Rheological measurements

The rheometer used was an Anton Paar MCR502 with a PP25/P2 samples plate and a Peltier H-PTD 200 temperature controlled hood.

2.3.6.1 *Technique*

Rheology is the study of the relationship between force (stress) and deformation (strain) of engineering materials under a set of loading and environmental conditions. It is considered a fundamental tool both in the process of control of the experimental gelation, as in the final characterization of the gels. The study of rheological parameters such as viscosity, shear stress or shear rate, are necessary to rheological and microstructural characterization of the gels [38].

The tests carried out in the rheometer were the following:

- Amplitude sweep tests (1, 5 y 10 rad/s): in order to determine the linear viscoelastic región of the sample.
- Frequency sweep tests: this provides more information about the effect of colloidal forces, the interactions among particles or droplets. In a frequency

sweep, measurements are made over a range of oscillation frequencies at a constant oscillation amplitude and temperature.

2.3.6.2 *Samples preparation for analysis*

Rheological tests were performed to characterize the properties of the HPMC-C_{12} hydrogel.

A sufficient quantity of gel was deposited in the plate destined for the placement of the samples, so that it was completely covered when the analysis began.

2.3.7 PLA-g-P(NIPAm-co-MAA) nanoparticles characterization

The PLA-g-P(NIPAm-co-MAA) is the final result of the three successive steps for the synthesis of the nanoparticles and, to verify the success of the nanoparticles obtained, ^{1}H-NMR, ^{13}C-NMR and organic GPC studies were carried out, as explained above.

From the NMR spectra, the peaks obtained were analyzed to determine the molecule produced and its molecular weight.

From the results of the GPC analysis, data on the average molecular weight and molecular weight distribution of the nanoparticles were obtained.

2.3.8 HPMC based hydrogels with organic nanoparticles drug release

For HPMC-based hydrogels, drug release experiments were performed in order to assess the amount of drug released and its influence on organic nanoparticles.

FITC was used as a drug simulator and the amount of drug released was analyzed by UV analysis.

To perform this UV analysis, the absorbance of the samples was measured at a wavelength of 440 nm, since FITC has a peak at that wavelength.

A calibration curve was also made to relate the absorbance obtained with the corresponding FITC concentration according to the Lambert-Beer's law (Equation 7):

$$Abs = \varepsilon \cdot b \cdot C \qquad \text{[Equation 7]}$$

Where:

Abs = absorbance of the solution at a given wavelength [-]

ε = molar extinction coefficient [$M^{-1} \cdot cm^{-1}$]

b = cuvette pitch length [cm]

C = solution concentration [M]

The calibration curve obtained was the following one:

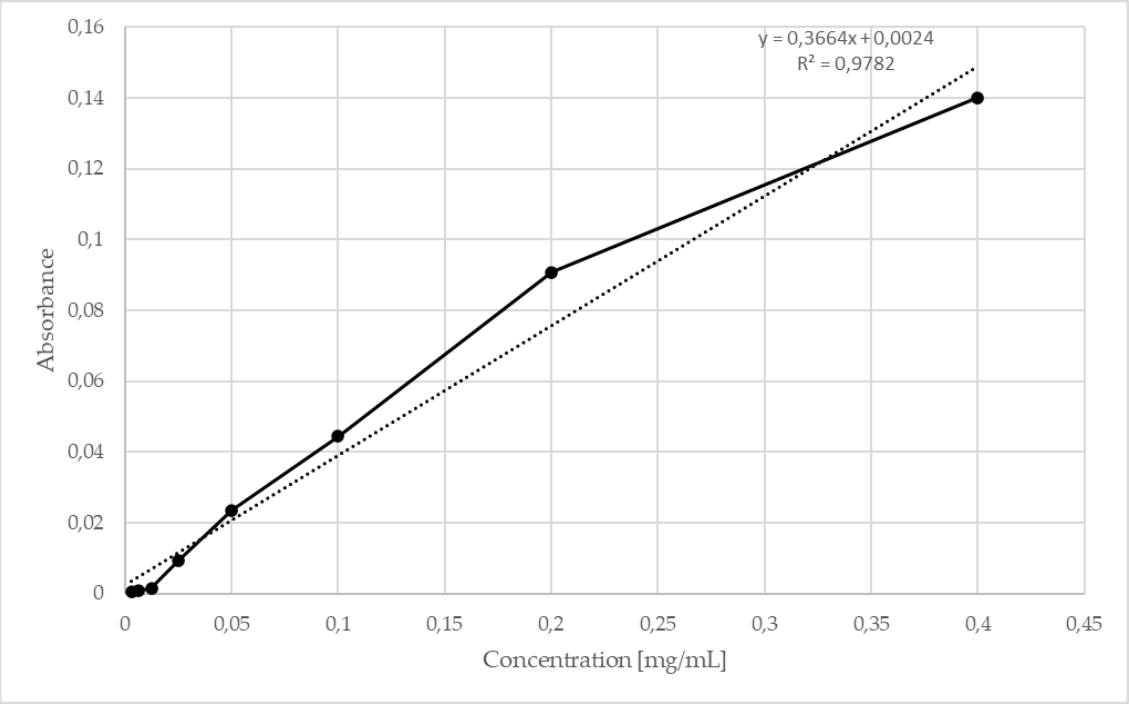

Figure 25: Calibration curve relating the absorbance of FITC to its concentration

The amount of drug released was evaluated from the cumulative release fraction [%]:

$$m_t = \frac{V \cdot C_t + \sum_{t=0}^{t-1} C_i \cdot V_{sample}}{m_0} \cdot 100 \qquad \text{[Equation 8]}$$

Where:

m_t = cumulative release fraction at time t

V = volume of the releasing media

C_i = concentration of FITC in the sample at time t

V_{sample} = volume taken at each time t

m_0 = total mass of FITC charged at t = 0 in the hydrogel

2.3.8.1 HPMC hydrogels drug release – Acidic environment pH 5.0 and 42 ºC

After the polymer-nanoparticles hydrogel union, the three membranes prepared were put in three Pyrex filled with 20 mL each of them with a H_2O adjusted to pH 5 by using HCl. The Pyrex were placed in a water bath at 42 ºC under stirring and wrapped in foil since the FITC loses its optical properties when exposed to light.

After the first 5 minutes, a wash was carried out, extracting the 20 mL of solution and adding other 20 mL. From that moment on, samples were taken progressively until reaching 1344 hours, extracting 10 mL each time and adding other 10 mL.

3. Results and discussion

3.1 PLA-g-P(NIPAm-co-MAA) nanoparticles synthesis products characterization

To characterize the synthesized nanoparticles, different analysis were performed at each stage, such as ^{1}H-NMR spectra, GPC or AFM analysis for the final nanoparticles.

3.1.1 Characterization of D,L-lactide

As a reference for the successive steps in the synthesis of the nanoparticles, a ^{1}H-NMR spectrum of D,L-lactide was performed. This spectrum is represented in Figure 26.

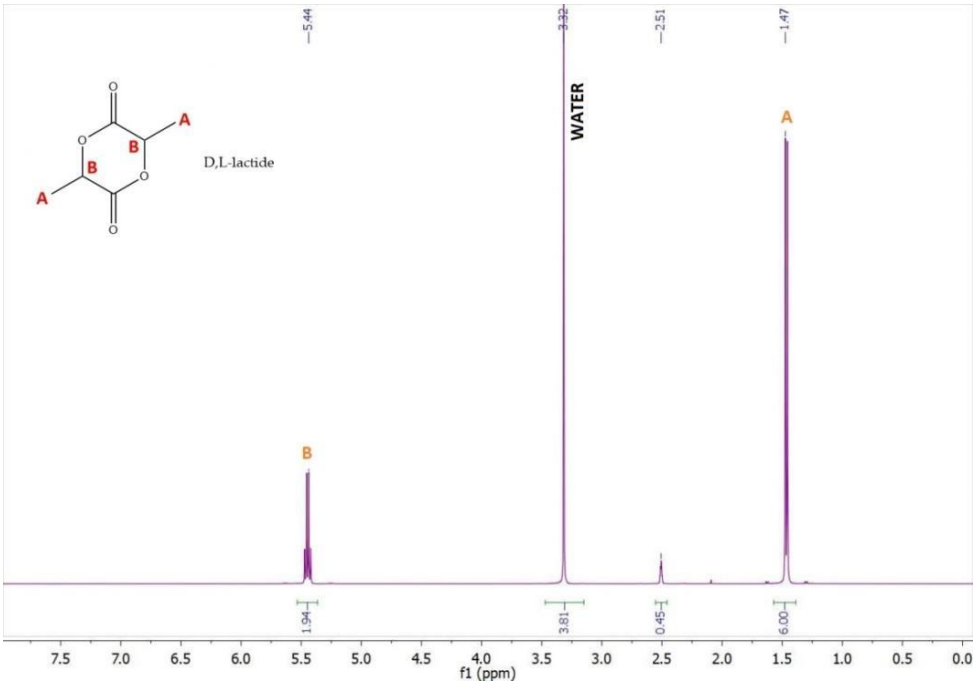

Figure 26: ^{1}H-NMR analysis of D,L-lactide

Four significant peaks are found in this spectrum:

- Peak at 3,32 ppm: this is the one related to water
- Peak at 5,44 ppm: this peak is related to the CH groups. Its integral is around the value of 2 because of the presence of 2 hydrogen atoms.
- Peak at 1,47 ppm: this last peak is related to the CH_3 groups. Its integral is of 6 because of the 6 hydrogen atoms, 3 of each group.
- Peak at 2,51 ppm: this peak corresponds to the DMSO-d6, the solvent used for the sample preparation.

3.1.2 Characterization of PLA

The polylactic acid (PLA) is the result of the first step of the nanoparticles synthesis. It consists on a Ring Opening Polymerization (ROP) reaction by using benzyl alcohol as the initiator and stannous octoate as a catalyst, terminating the reaction by adding a certain amount of methanolic KOH.

For the characterization of PLA, a ^{1}H-NMR and a GPC were performed.

3.1.2.1 ^{1}H-NMR analysis

For the PLA ^{1}H-NMR analysis, DMSO-d6 was used as solvent. The obtained spectrum is reported in Figure 27.

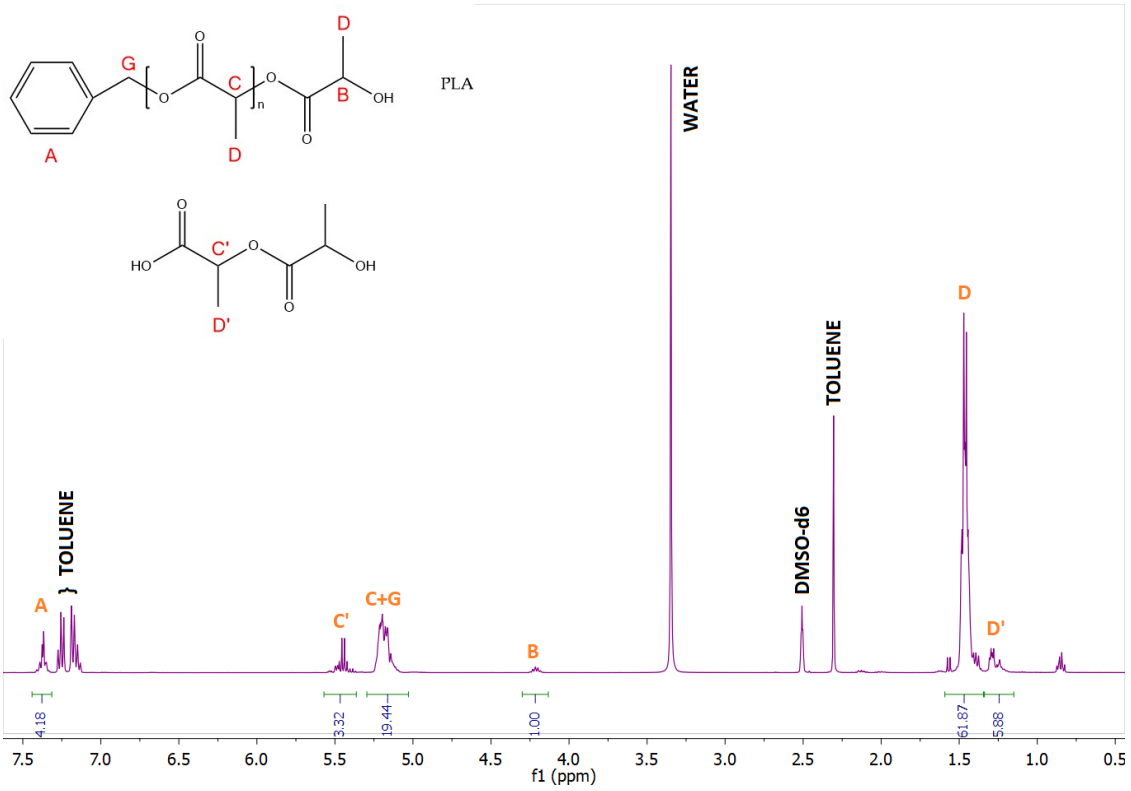

Figure 27: ^{1}H-NMR analysis of PLA

In this spectrum there are different significant peaks:

- A peak: this peak is obtained at 7,37 ppm of the spectrum, and it is related to the hydrogen atoms of the benzyl group, so its integral is around the value of 5.
- C' peak: this peak is found at 5,44 ppm an it is related to the presence of the dilactic acid produced from the ring opening of the D,L-lactide.
- C+G peaks: these group of peaks found around 5,20 ppm and the sum of their integrals results around 20. This value gives the number of repeating units within the polymer.
- B peak: it is found at 4,20 ppm in the spectrum and it represents the single hydrogen atom of the CH group at the end of the chain. Because of this reason, its integral value is 1.
- D peak: this peak, found at 1,47 ppm, is associated to the CH_3 group of the repeating unit, so it should be around three times the value of peak C+G. It turns around 61.
- D' peak: it is found at 1,28 ppm and is also related to the presence of the dilactic acid produced from the ring opening of the D,L-lactide.
- Toluene peaks: there are three peaks at 7,26 ppm, 7,14 ppm and 2,30 ppm, which are the characteristic peaks of toluene in DMSO-d6.
- Water peak: the water peak is found at 3,35 ppm.
- DMSO-d6 peak: the peak at 2,51 ppm is the one related to the DMSO-d6 used as solvent.

3.1.2.2 GPC analysis

To perform the second step of the nanoparticles synthesis, it is necessary to obtain the molecular weight of the PLA, so an organic GPC analysis reported in Figure 28 was performed.

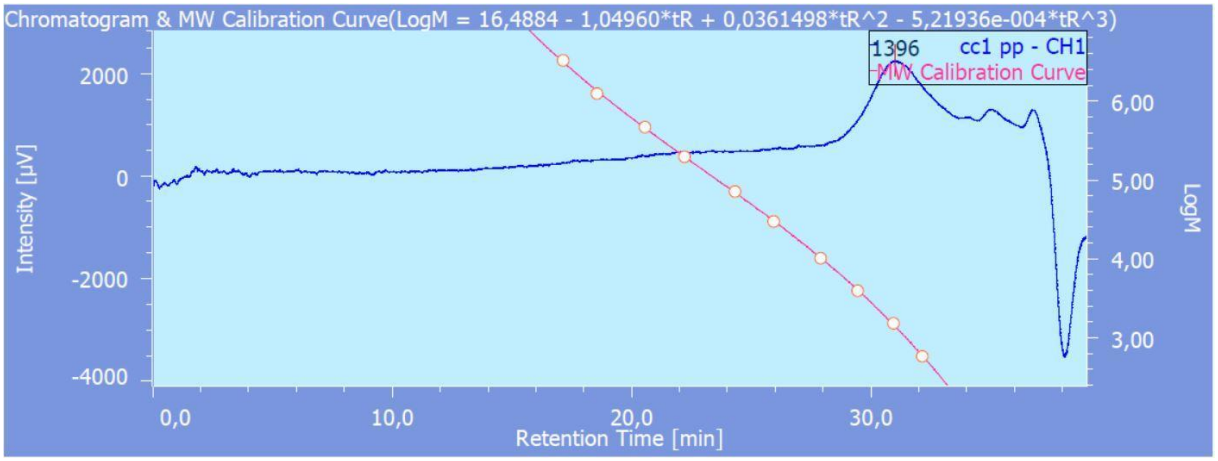

Figure 28. Chromatogram of organic GPC analysis of PLA

The predominant peak obtained was the first one with a higher intensity. From this peak it can be obtained the retention time (t_r) and the molecular weights of the polymer synthesized. To do so, the instrument should be well calibrated. The polymer that has been used for the calibration of the instrument is polystyrene at different molecular weights, which differs from the structure of the polymer analysed.

The data obtained from the GPC analysis is reported in Table 5.

Table 5. GPC results of PLA

	t_r	M_p	M_n	M_w	M_w/M_n
#1	30,99	1396	987	1583	1,604

As have been seen in the GPC theory, the polymer chains with higher molecular weights exit preferentially with a lower tr, while those with lower molecular weights, go through the column following a longer path before the exit.

As can be seen in Table 5, the t_r obtained was of 30,99 min. The molecular weight obtained was of 987 g/mol, and it was the one used to perform the second part of the synthesis.

3.1.3 Characterization of PLA-MA

The second step in the nanoparticles synthesis was the methacrylic group addition to the PLA. The PLA product from the ROP reaction underwent further esterification reaction with methacryloyl chloride (MACl) to obtain the macromonomer, PLA-MA.

To characterize the product, a ^{1}H-NMR and a GPC analysis were performed.

3.1.3.1 ^{1}H-NMR analysis

In the PLA-MA synthesis, a ^{1}H-NMR analysis was performed before and after the purification steps. DMSO-d6 was used as solvent and the spectrums obtained are reported in Figure 29 and Figure 30, respectively.

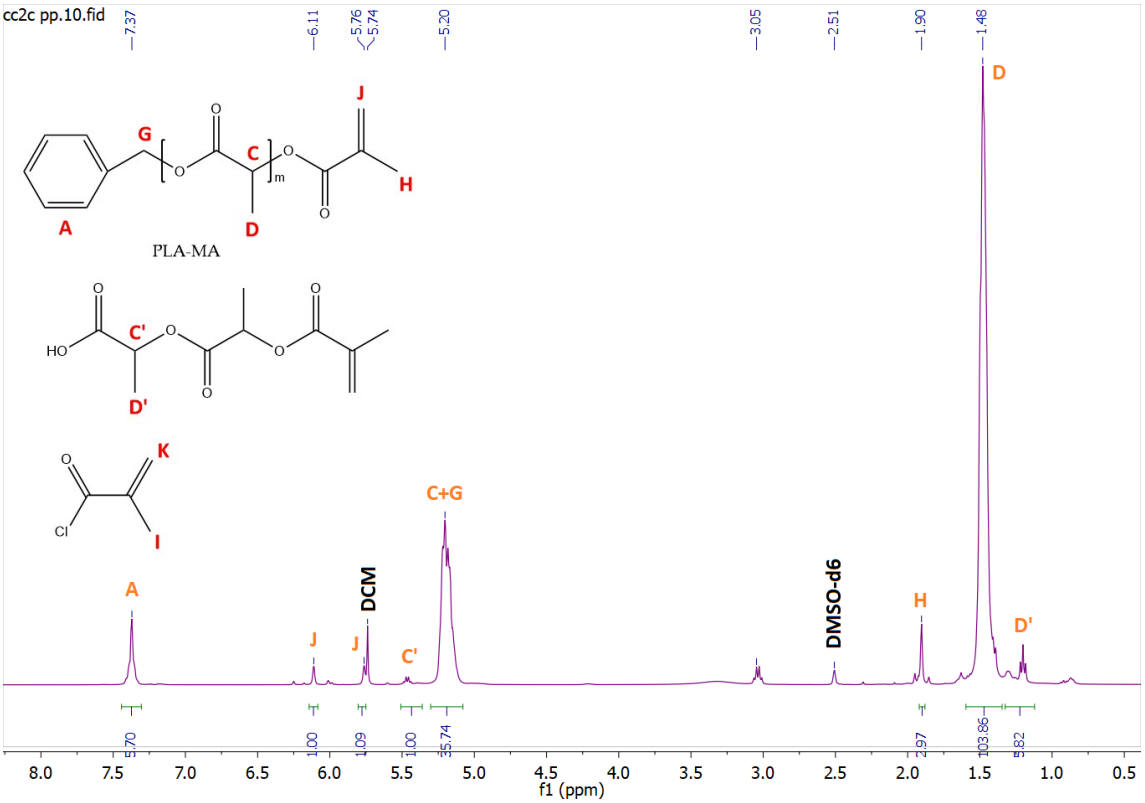

Figure 29: ^{1}H-NMR analysis of PLA-MA before purification

In this spectrum there are some significant peaks to be analysed:

- A peak: this peak is obtained at 7,42 ppm of the spectrum, and it is related to the hydrogen atoms of the benzyl group, so its integral is around the value of 5.
- K peaks: they correspond to the unreacted methacryloyl chloride and are found at 6,31 ppm and 6,08 ppm.
- I peaks: there are two peaks referred to the methacrylic group of the product obtained, one of them at 6,16 ppm and 5,82 ppm. They are associated with the two hydrogen atoms of the CH_2 group. This is the reason why the sum of its integrals is around 2.
- C' peak: this peak is found at 5,51 ppm an it is related to the presence of the dilatic acid which hasn't polimerized but just opened in the ring opening of the D,L-lactide.
- C+G peaks: these group of peaks found around 5,26 ppm and the sum of their integrals results around 26. This value gives the number of repeating units within the polymer.
- I peak: it is found at 2 ppm and it corresponds to the unreacted MACl.
- H peak: they also refer to the methacrylic group, found at 1,95 ppm. It is related to the CH_3 group, so its integral is around 3.
- D peak: this peak, found at 1,53 ppm, is associated to the CH_3 group of the repeating unit, so it should be around three times the value of peak C+G. It turns around 74.
- D' peak: it is found at 1,20 ppm and is also related to the presence of the dilactic acid which hasn't polimerized but just opened in the ring opening of the D,L-lactide.
- Toluene peaks: there are three peaks at 7,31 ppm, 7,23 ppm and 2,36 ppm, which are the characteristic peaks of toluene in DMSO-d6. It appears as a residue of the solvent used during the synthesis.
- Water peak: the water peak is found at 3,37 ppm.
- DMSO-d6 peak: the peak at 2,56 ppm is the one related to the DMSO-d6 used as solvent.

The unreacted compounds should disappear in the purification step before the copolymerization final stage. The ^{1}H-NMR spectrum after purification is reported in Figure 30.

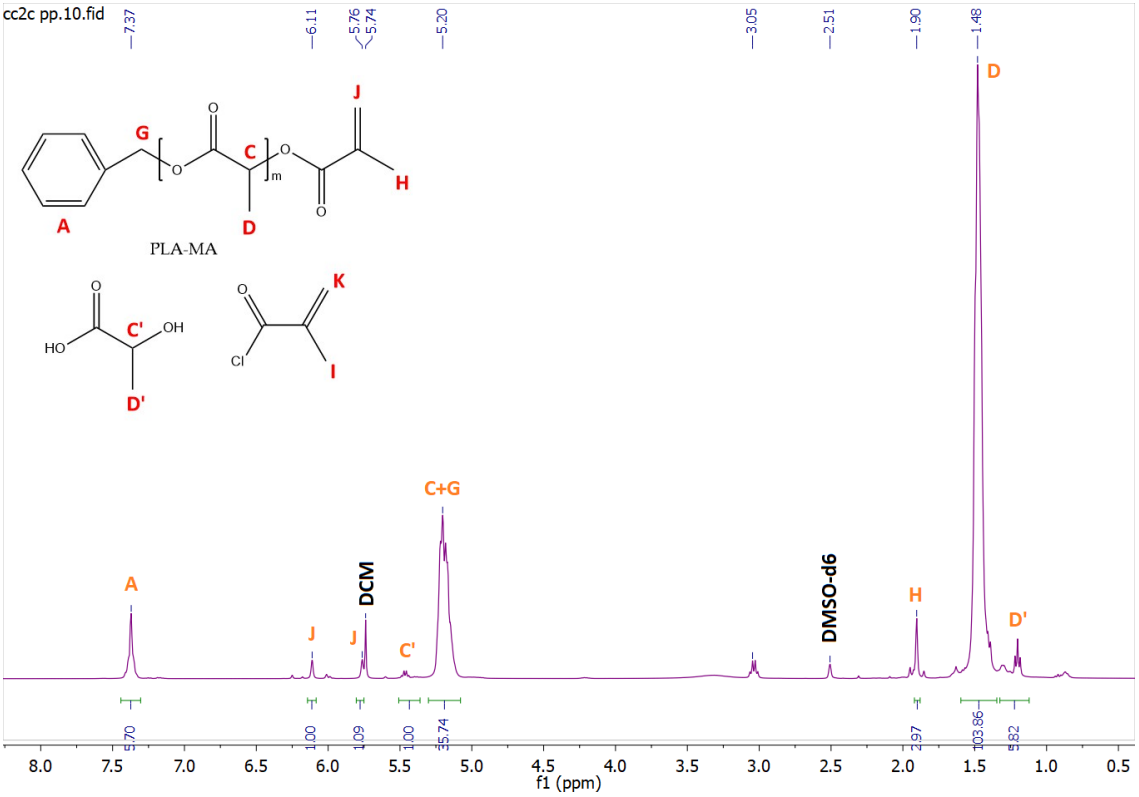

Figure 30: ^{1}H-NMR analysis of PLA-MA after purification

During the purification of the product, a precipitation in hexane was performed in order to remove the methacryloyl chloride (MACl). In Figure 30 the peaks related to the MACl, the unreacted compound and the solvents used in the synthesis no longer appear.

The rest of the peaks reported on the spectrum are the same obtained before the purification step.

3.1.3.2 GPC analysis

As done for the PLA synthesis product, an organic GPC was performed for the PLA-MA in order to obtain the molecular weights to correctly perform the last step of the nanoparticles synthesis.

The chromatogram obtained is reported in Figure 31.

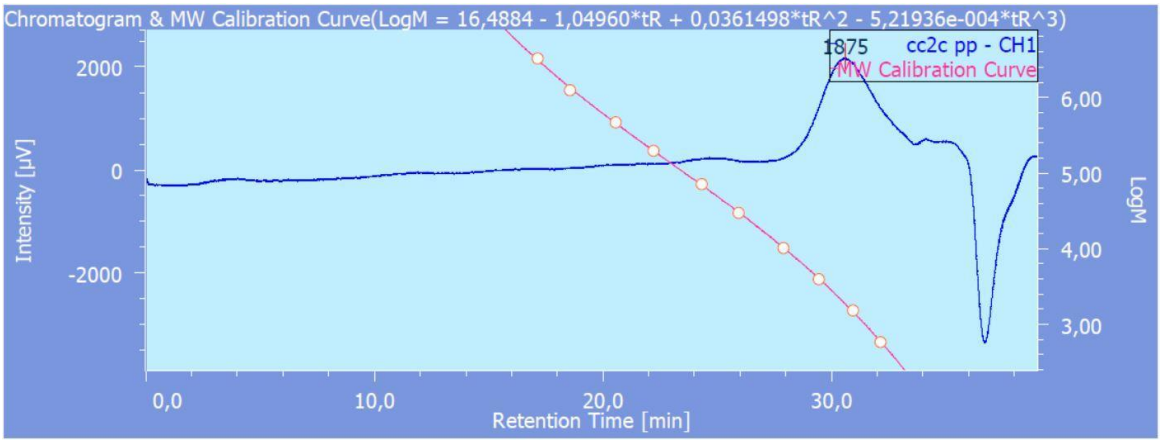

Figure 31. Chromatogram of organic GPC analysis of PLA-MA

The peak obtained was the one with the highest intensity. From this peak it can be obtained the retention time (t_r) and the molecular weights of the polymer synthesized. The polymer that has been used for the calibration of the instrument is polystyrene at different molecular weights, which differs from the structure of the polymer analysed.

The molecular weight of the PLA-MA is reported in Table 6.

Table 6. GPC results of PLA-MA

	t_r	M_p	M_n	M_w	M_w/M_n
#1	30,57	1875	1192	2072	1,7384

As can be seen in Table 6, the t_r obtained was of 30,57 min. The molecular weight obtained was of 1192 g/mol, and it was the one used to perform the last part of the synthesis.

3.1.4 Characterization of PLA-g-P(NIPAm-co-MAA)

The last step in the nanoparticles synthesis was the copolymerization reaction. To characterize the product, a ^{1}H-NMR and an organic GPC analysis were performed.

3.1.4.1 ^{1}H-NMR analysis

In the PLA-g-P(NIPAm-co-MAA) synthesis, a conventional free radical polymerization was performed to obtain the copolymer with PLA-MA, NIPAm and AIBN as initiator of the reaction.

A ^{1}H-NMR analysis was performed. DMSO-d6 was used as solvent and the spectrum obtained is reported in Figure 32.

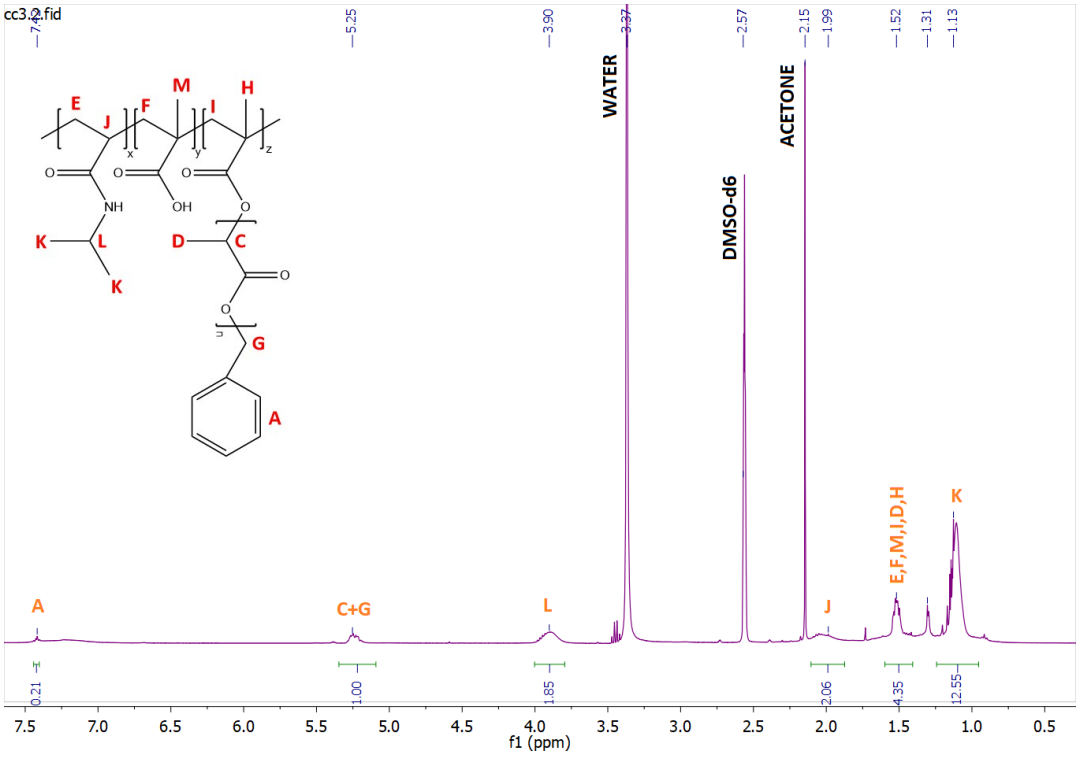

Figure 32. ^{1}H-NMR analysis of PLA-g-P(NIPAm-co-MAA)

The characteristic peaks of the PLA-g-P(NIPAm-co-MAA) spectrum were the following:

- A peak: this peak is obtained at 7,42 ppm of the spectrum, and it is related to the hydrogen atoms of the benzyl group.
- C+G peaks: these group of peaks found around 5,25.
- L peak: it is referred to the las CH group of the NIPAm, found at 3,90 ppm. So its integral is around 2.
- J peak: this peak, found at 1,99 ppm, is associated to the CH group of the chain linked to the NIPAm.
- E, F, M, I, D, H peaks: they are found at 1,52 ppm and they are related to the CH_2 and CH_3 groups.
- K peak: found at 1,13 ppm and is related to the CH_3 groups of the NIPAm molecule.
- Water peak: water peak is found at 3,37 ppm.
- DMSO-d6 peak: the peak at 2,57 ppm is the one related to the DMSO-d6 used as solvent.
- Acetone peak: found at 2,15 ppm is the one associated with the acetone used as solvent in the synthesis.

3.1.4.2 GPC analysis

An organic GPC analysis of the copolymer was carried out with the results reported in Figure 33.

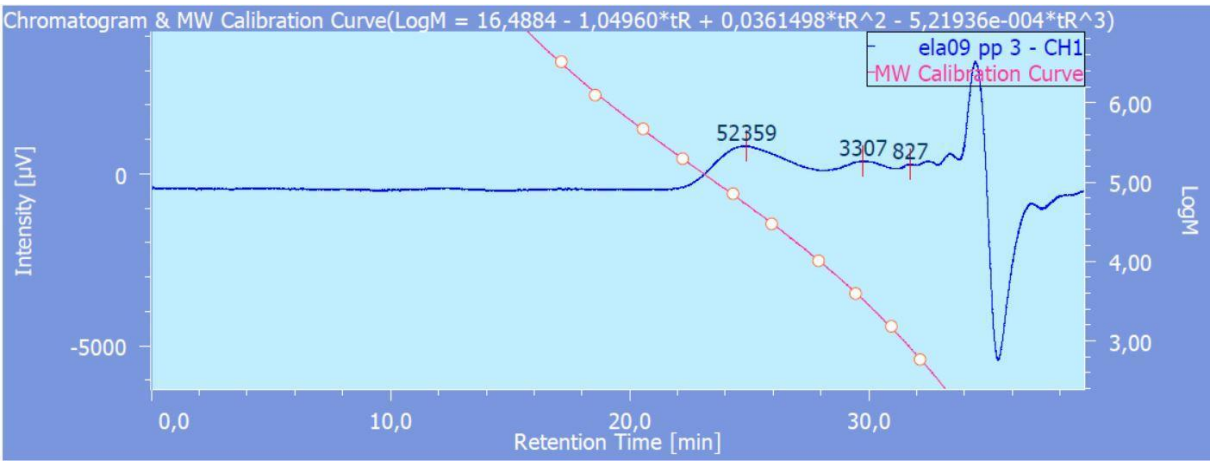

Figure 33. Chromatogram of organic GPC analysis of PLA-g-P(NIPAm-co-MAA)

Three peaks are identified before the solvent peak. The highest intensity occurs for the first peak. Table 7 shows the retention times t_r and the molecular weights obtained with an appropriate calibration of the instrument. The polymer used for calibration is polystyrene at different molecular weights, which differs in part from the structure of the copolymer analysed.

Table 7. GPC results of PLA-g-P(NIPAm-co-MAA)

	t_r	M_p	M_n	M_w	M_w/M_n
#1	24,85	52359	46272	60656	1,31
#2	29,73	3307	3098	3525	1,138
#3	31,69	827	847	855	1,009

M_w/M_n is the polydispersity value, the closer it is to 1, the more monodisperse the polymer is; the more detached it is, the more polydisperse the polymer is.

All the peaks correspond to copolymers with different molecular weight, but also the first one will remain trapped and will form the nanoparticles. It has a retention time of 24,85 min and a molecular weight of 46272 g/mol.

3.2 Characterization of nanoparticles

For the nanoparticles characterization after the dialysis of PLA-g-P(NIPAm-co-MAA), a ^{1}H-NMR, a DLS analysis and an AFM analysis were performed.

3.2.1 ^{1}H-NMR analysis

The nanoparticles were formed as a result of PLA-g-P(NIPAm-co-MAA) dialysis and were analyzed by ^{1}H-NMR spectrum using deuterium oxide (D_2O) as solvent.

This spectrum is shown in Figure 34.

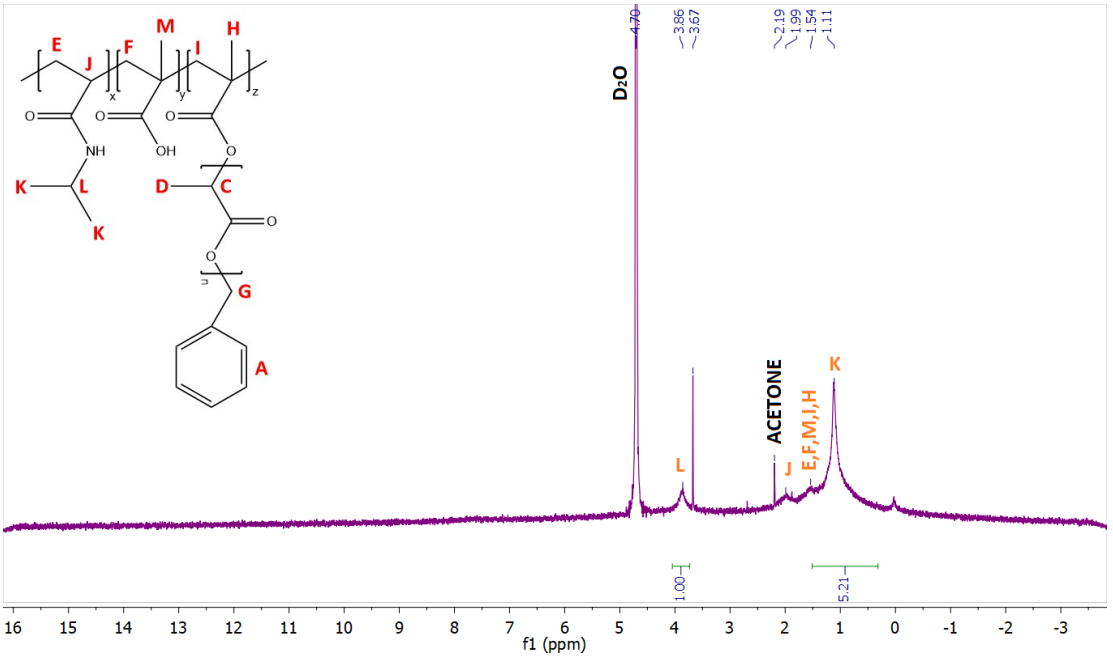

Figure 34. ^{1}H-NMR analysis of PLA-g-P(NIPAm-co-MAA) nanoparticles after dialysis in distilled water

What is observed in this spectrum is that, after dialysis, the peaks corresponding to the hydrophobic chains no longer appear. This fact confirms the successful formation of nanoparticles with hydrophobic terminal groups facing inwards, and hydrophilic terminal groups facing outwards (Figure 34).

3.2.2 DLS analysis

DLS analysis was performed in order to obtain the size of the nanoparticles and analyze their variation with temperature. The results obtained are represented in Table 8 and Figure 35.

Each analysis was performed three times and the average size was obtained.

Table 8. Particles average size change with respect to the temperature

T (ºC)	Average Size (d.nm)
20	1361,83
21	649,90
22	848,10
23	917,60
24	1005,37
25	1077,07
26	1181,13
27	1064,30
28	1137,60
29	1130,47
30	1117,30
31	1058,43
32	1220,90
33	1265,67
34	1104,67
35	1212,00
36	1050,13
37	1146,93
38	1135,80
39	1097,13
40	1300,33
41	1703,33
42	1618,33
43	1370,50
44	1209,03
45	976,50

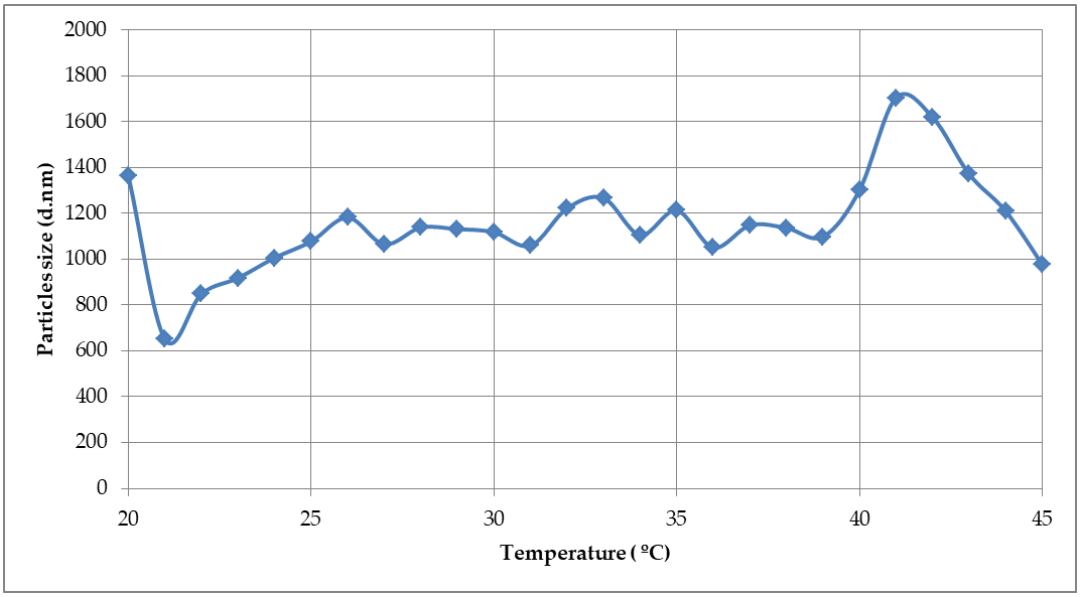

Figure 35. DLS analysis of average particle size with respect to the temperature

According to the literature studied, as the temperature increases, a decrease in the size of the particles should be expected, since they have a thermo-responsive behavior.

Contrary to what was expected there is no change in dimension with temperature, so nanoparticles cannot be considered thermo-responsive. For this reason the analysis should be repeated to verify such behavior. This may be due to the fact that the particles have not completely formed or due to a problem during the analysis.

Another DLS analysis was performed analyzing only the samples at 37 ºC and 42 ºC. They were analyzed three times and the results obtained are reported in Table 9:

Table 9. Single DLS analysis for 37 ºC and 42 ºC

T (ºC)	Average Size (d.nm)	Standard Deviation (d.nm)
37	**2003,33**	388,40
42	**1316,33**	213,63

As can be observed, in this experiment, a notable change in particle size is shown as a function of temperature, decreasing approximately 700 nm between 37 ºC and 42 ºC.

3.2.3 AFM analysis

An AFM (Atomic Force Microscopy) analysis produces images with near-atomic resolution to measure the surface topography. AFM analysis is capable of quantifying sample surface roughness down to the angstrom scale, as well as providing quantitative measurements of feature sizes such as step height and other dimensions [40].

In this case, the AFM analysis was done to assess the size and topographic profile of the nanoparticles obtained.

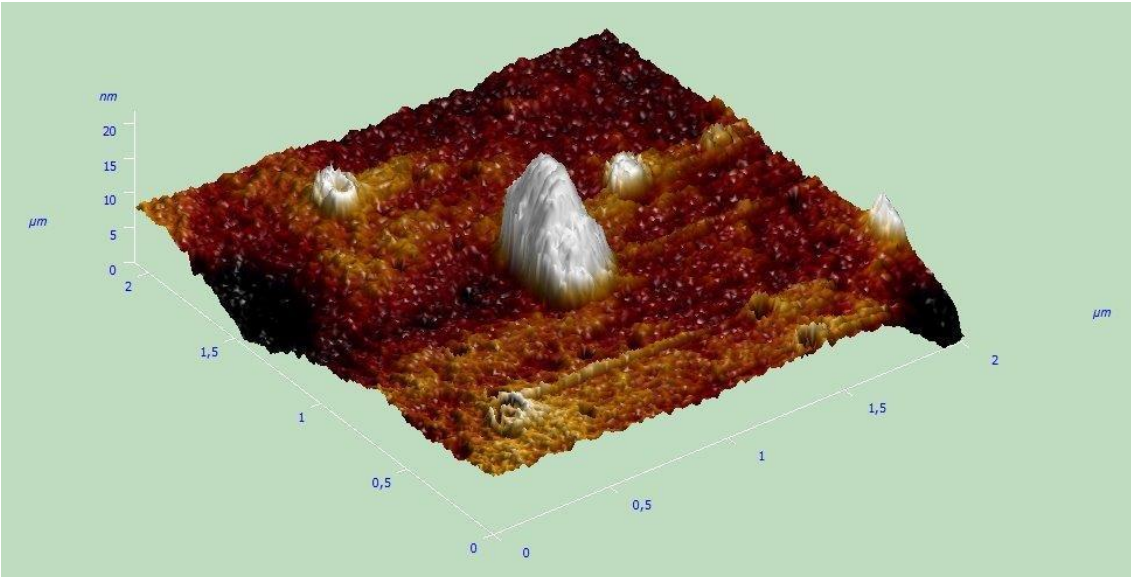

Figure 36. Reconstruction of the three-dimensional profile of a nanoparticle

Figure 36 shows a study area of 2 µm x 2 µm in which some higher points of the analyzed surface stand out, which correspond to the presence of a particle. On the other hand, the darkest areas of the surface represent holes in which no solvent residues remain.

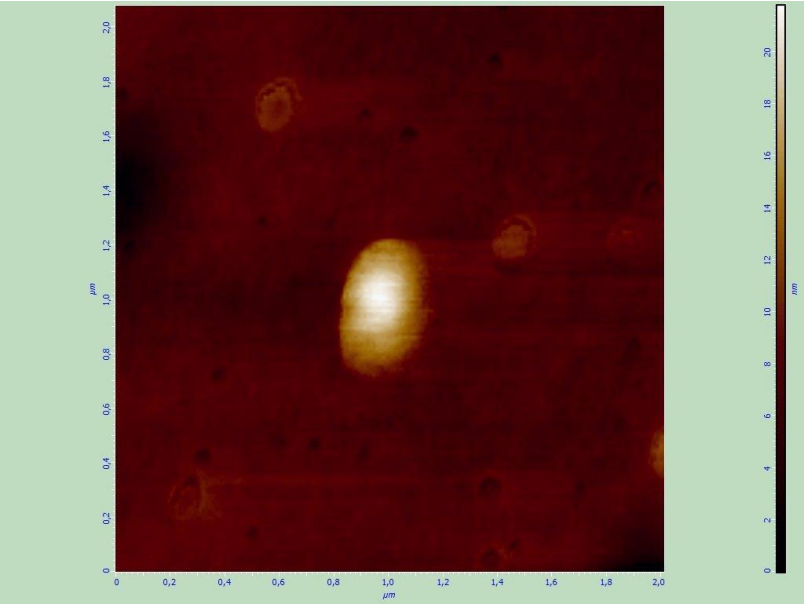

Figure 37: AFM image in 2D representation

In this case, Figure 37 shows a 2D image of the previously analyzed three-dimensional reconstruction. Also in this case a more luminous zone is observed that represents the presence of a particle. In the same way, the dark areas correspond to the areas where there are no solvent residues. The nanoparticle observed is located in the centre of the surface, at a 1 µm distance on both axes.

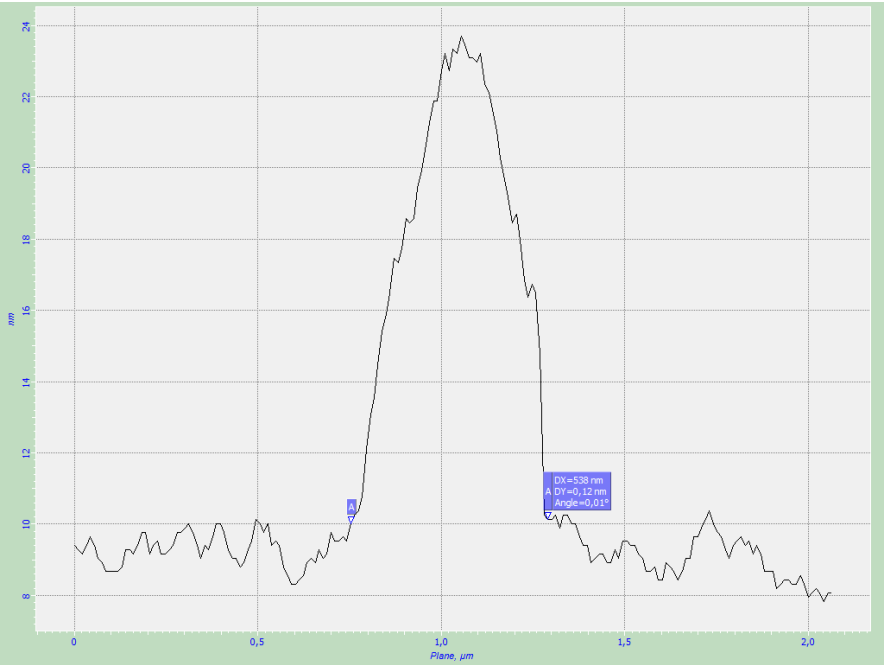

Figure 38. Y axis profile

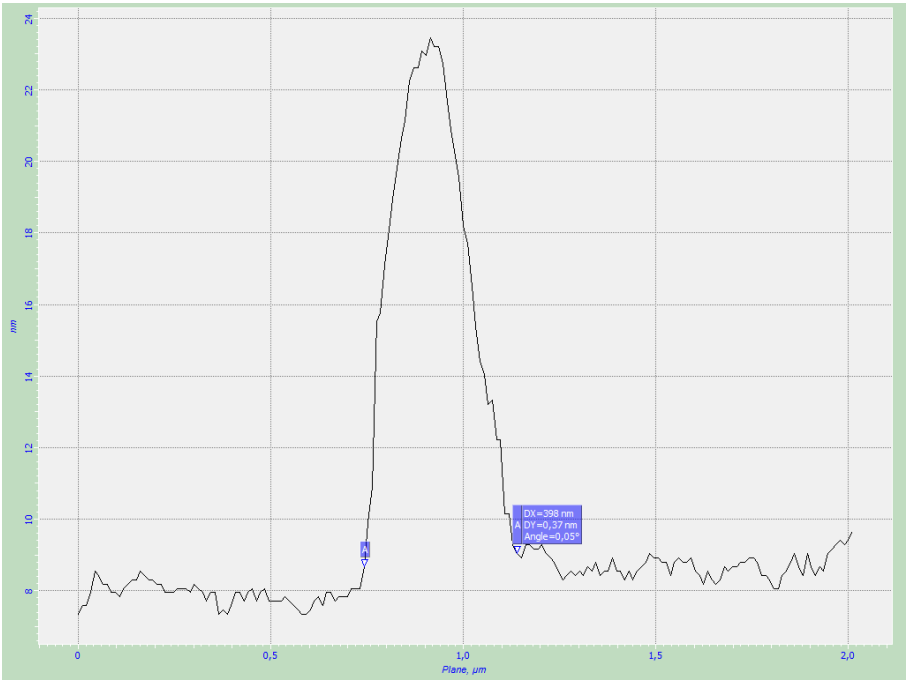

Figure 39. X axis profile

As have been observed in previous figures, the nanoparticle is located in the centre of the analysed surface, so Figure 38 and Figure 39 show the topographic profile of the selected area in the two axes passing through the central point of the plot.

From the images obtained by AFM analysis, it is possible to assess that the size of the nanoparticles is of 520 nm x 380 nm. On the other side, the height of the particles that can be seen from the profile is of approximately 15 nm.

The data has been measured from the images using ImageJ software.

The visible particle shape is influenced by the fact that the sample was heated to evaporate the solvent before the AFM analysis.

3.3 HPMC-C_{12} hydrogel characterization

The functionalization of HPMC was performed by dissolving HPMC in N-methylpyrrolidone and mixing the solution with 1-dodecylisocyanate.

For the HPMC-C_{12} hydrogel characterization, a FT-IR and a SEM analysis within some rheology tests were performed.

3.3.1 FT-IR analysis

The FT-IR analysis was performed as a comparison between HPMC and HPMC-C_{12}, the spectrum obtained is shown in Figure 40.

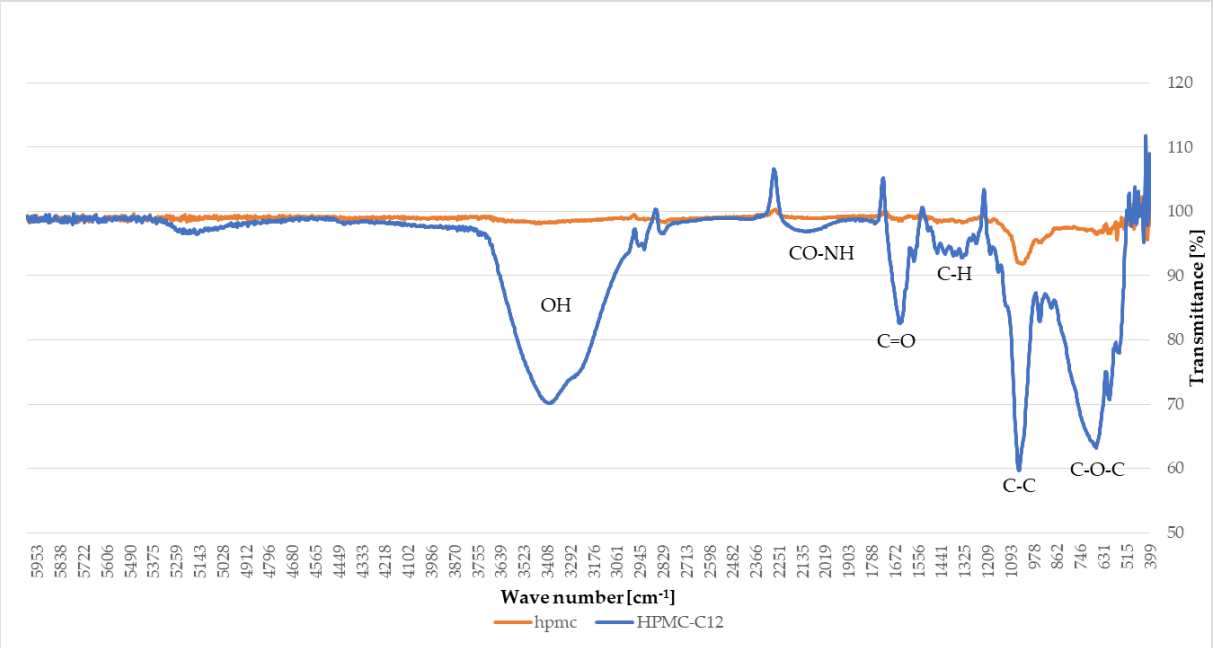

Figure 40. FT-IR spectrum for HPMC and HPMC-C_{12} comparison

As observed in Figure 40, there are some significant peaks to be analysed:

- OH peak: this peak is found at, aproximately, 3400 cm^{-1}, and corresponds to the vibration and stretching of the –OH groups [20].

- CO-NH peak: found around 1150 cm^{-1} is the corresponding to the CO-NH of the functionalized part of HPMC-C_{12}.
- C=O peak: characteristic absorption band of C=O bonds normally found around 1700-1650 cm^{-1} [43].
- C-H peak: found between 1400-1350 cm^{-1}, it represents the symmetrical vibration of C-H bonds; while the region between 1500-1450 cm^{-1} represents the asymmetric vibration out of phase of C-H bonds [20].
- C-C peak: found around 1000 cm^{-1}, characteristic of C-C bonds.
- C-O-C peak: at 650 cm^{-1}, characteristic of C-O-C bond of HPMC [20].

3.3.2 SEM analysis

The Scanning Electron Microscopy (SEM) consists of an emission of a scanning electron beam on the sample. These electrons interact with the sample producing different signals that are collected in detectors that subsequently transform them to give a high-definition image of the topography of the surface of our sample [41].

The SEM analysis was performed for both the HPMC-C_{12} hydrogel with and without nanoparticles, shown in Figure 41 and Figure 42.

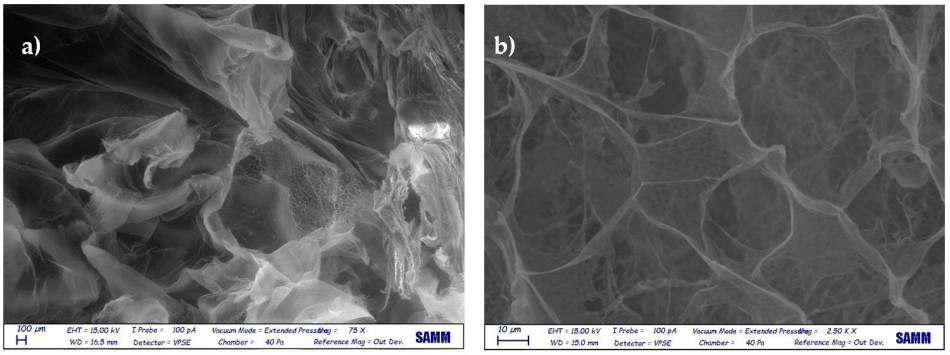

Figure 41. SEM images of HPMC-C_{12} hydrogel without NPs at different magnifications: a) 100 μm; b): 10 μm

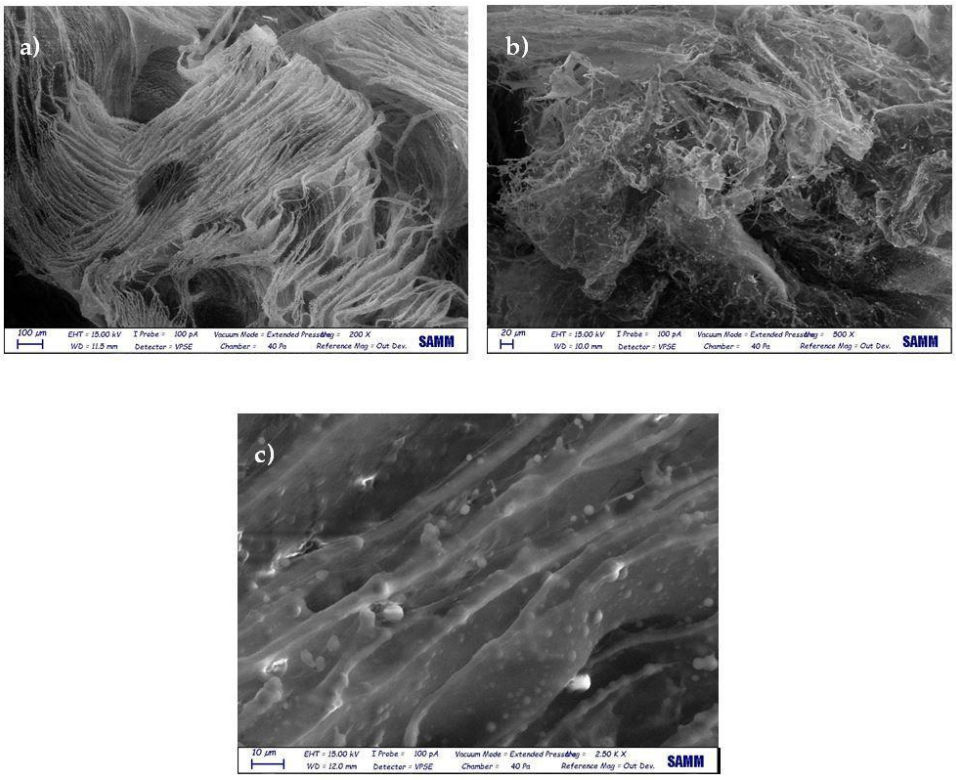

Figure 42. SEM images of HPMC-C_{12} hydrogel with NPs at different magnifications: a) 100 μm; b): 20 μm; c) 10 μm

In the images of the SEM analysis obtained, the appearance and shape of the hydrogel can be observed at different microscope magnifications. The main difference is that before the nanoparticles are introduced, the surface of HPMC-C_{12} is smoother. When mixing the nanoparticles with the gel, these nanoparticles are observed in all magnifications as small spheres well adhered to the gel structure (Figure 41 and Figure 42).

3.3.3 Rheology tests

The rheological tests performed on the HPMC-C_{12} hydrogel were the amplitude sweep and the frequency sweep.

3.3.3.1 Amplitude sweep test

The objective of an amplitude sweep test is to determine the linear viscoelastic region of the material by describing how a material deforms and what happens when its structure breaks.

G' and G'' are known as storage or elastic moduli, and loss or viscous modulus, respectively. On the one hand, the elastic modulus (G') is associated with the energy stored in the material, while the viscous modulus (G'') is associated with the energy dissipated by the material.

When the elastic modulus (G') is greater than the viscous modulus (G''), the material behaves like a gel or a solid structure, and can be defined as a viscoelastic solid material. As the % Shear Strain increases, the elastic modulus increases until it reaches the limiting linear viscoelastic region (LVER). At that moment, both values of G'' and G' converge. From that point on, G'' becomes greater than G' and the sample behaves as a fluid structure called a viscoelastic liquid.

Said tests were carried out at different speeds (10 rad/s and 1 rad/s) and defining different percentages of minimum Shear Strain (0,01% and 0,001%), as shown in Figure 43, Figure 44 and Figure 45.

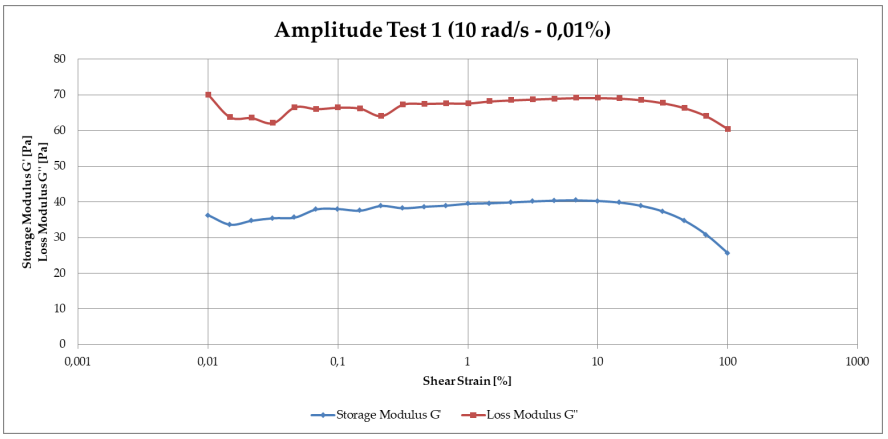

Figure 43. Amplitude sweep test (10 rad/s – 0,01 % minimum deformation)

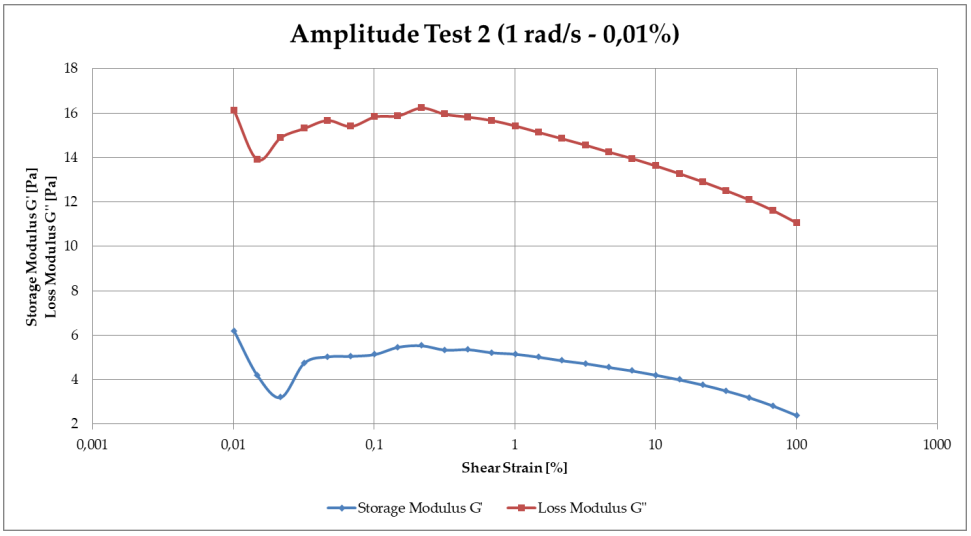

Figure 44. Amplitude sweep test (1 rad/s – 0,01 % minimum deformation)

As can be seen in the amplitude tests carried out (Figure 43, Figure 44 and Figure 45), the material does not behave as expected. Since the values of G'' are greater than those of G' throughout the test, it is known that the material does not behave like a gel, but like a solution. The only thing that can be observed is the transition from a linear behavior to a non-linear one (Figure 43) starting from a 10% shear strain, but without any crossover that indicates the transition from a solid-like material to a liquid-like material. Moreover, there is a breakdown of the internal structure of the material.

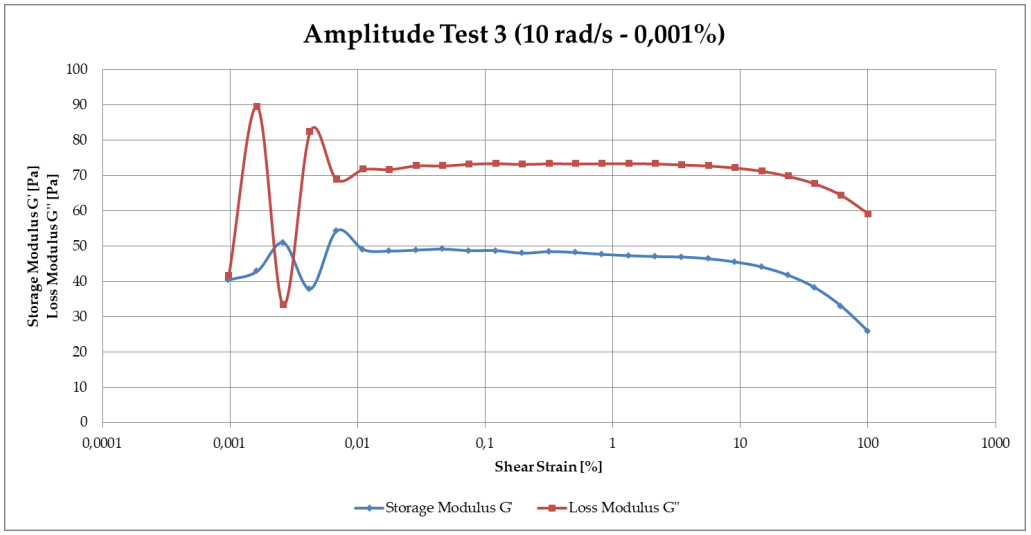

Figure 45. Amplitude sweep test (10 rad/s – 0,001 % minimum deformation)

As for the initial data (Shear Strain between 0,001% and 0,01%) at low deformation amplitudes the mechanical response of the material is at the limit of resolution of the instrument (Figure 45), as can be seen by the continuous oscillations at the beginning of the graph.

3.3.3.2 *Frequency sweep test*

A frequency sweep is a test used to determine the viscoelastic properties of a sample as a function of a time scale over a non-destructive strain range. It generates a unique rheological spectrum of each material.

Prior to the frequency sweep test, an amplitude sweep test should be performed to determine the limit of the linear viscoelastic region (LVER). In this type of test, the value of Shear Strain is kept constant at 0,02%.

The results obtained are shown in Figure 46.

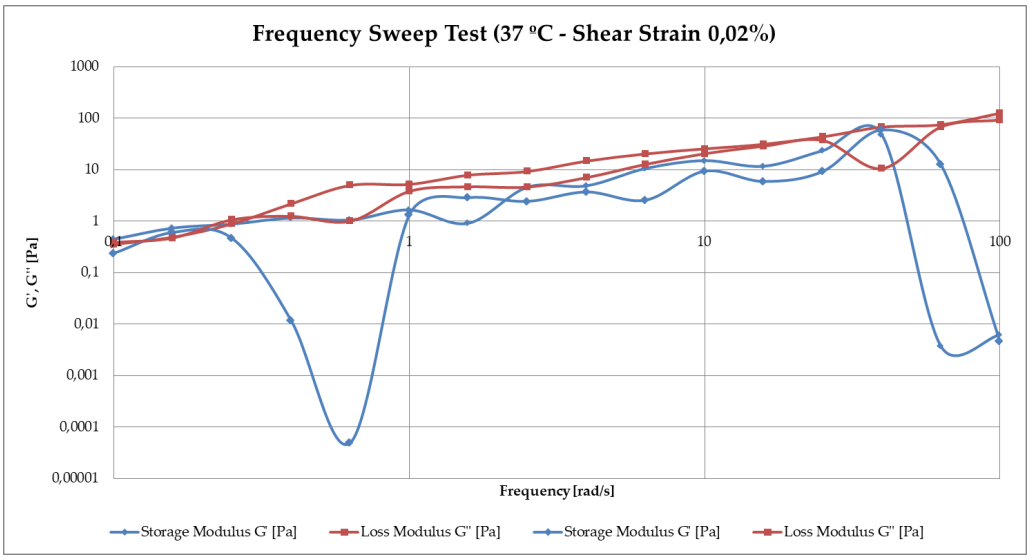

Figure 46. Frequency sweep test at 37 ºC

The two values are similar, but G' turns out to be always lower than G'', indicating a non-crosslinked material. Except at very low frequencies, where G' is slightly larger than G''. In addition, the values are low, so the mechanical properties of the material are very weak.

3.4 Drug release from polymer-nanoparticles HPMC-C_{12} hydrogels

To verify the release efficiency of organic nanoparticles in HPMC-C_{12} hydrogels, a drug release experiment was carried out in which the amount of drug simulant (FITC) released in an acidic aqueous medium (pH 5) was measured at 42ºC. This amount was obtained by UV spectroscopy and the percentage of drug released was defined as the ratio between the amount released and the total amount of drug loaded in the system (Equation 9 and Equation 10).

$$Drug\ mimetic\ laoded\ [\%] = \left(1 - \frac{m_{drug\ mimetic\ in\ cleaning\ water}}{m_{drug\ mimetic\ added}}\right) \cdot 100 \qquad \text{[Equation 9]}$$

$$Cumulative\ Release\ [\%] = \left(\frac{\sum_{t=0}^{t=i} m_{drug\ mimetic}}{m_{drug\ mimetic\ loaded}}\right) \cdot 100 \qquad \text{[Equation 10]}$$

Table 9 and Figure 46 show the percentages of cumulated drug release of FITC at 42ºC from the PLA-g-P(NIPAm-co-MAA) nanoparticles loaded inside the HPMC-C_{12} hydrogel.

Table 10. Quantity of FITC loaded for the release test

Temperature (ºC)	**Drug mimetic**	**Loading (mg)**	**Loading (%)**
42	FITC	2,002	77,25

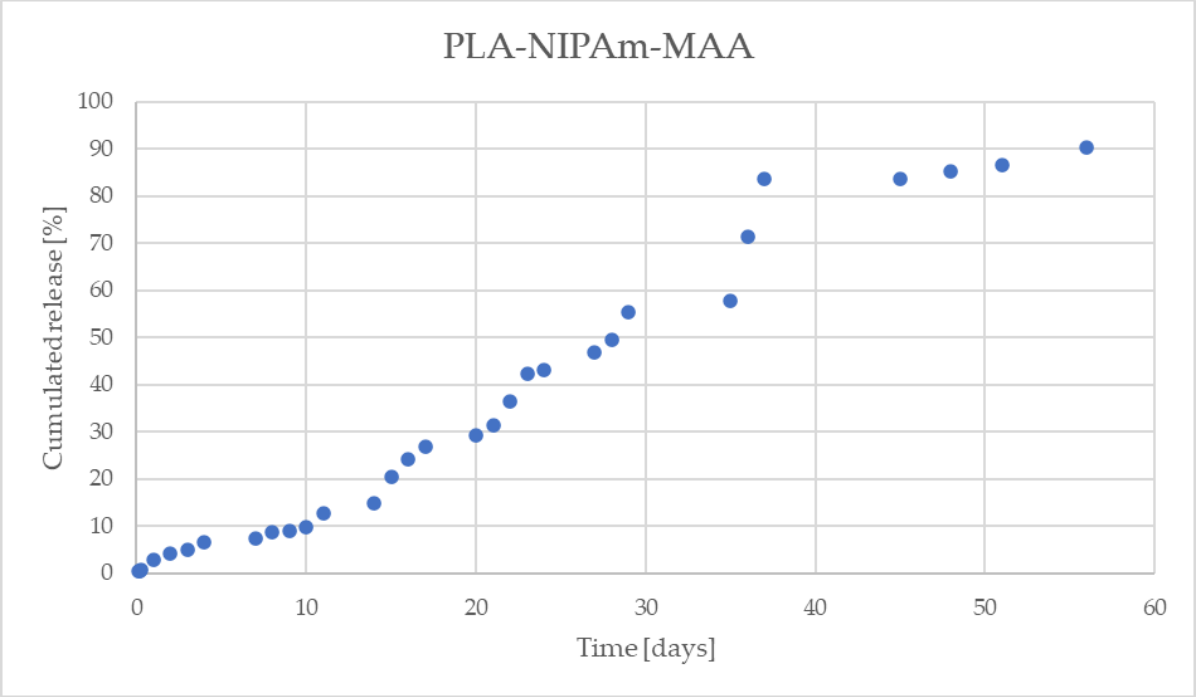

Figure 47. FITC release by PLA-g-P(NIPAm-co-MAA) nanoparticles at 42 °C in acidic environment (pH 5)

From Figure 47 it can be seen the increasing trend of the drug release within the time, reaching a plateau from approximately day 38, once 90% of drug released has been reached. This plateau is what makes the drug release controlled.

It is also observed that the time taken to reach 90% drug release is very high (1344 hours), this may be due to the fact that it is a hydrophobic molecule inside a hydrophobic core and it is released in an aqueous environment.

4. Conclusions

PLA-g-P(NIPAm-co-MAA) organic nanoparticles were synthesized and characterized, as well as the HPMC-C_{12} hydrogel by different analysis techniques. Furthermore, the nanoparticles were encapsulated in the hydrogel. This system was also characterized and studied using different analysis techniques.

Regarding the organic nanoparticles, the synthesis consisted of three stages that were carried out until the copolymer PLA-g-P(NIPAm-co-MAA) was successfully obtained. It was synthesized by a first Ring Opening Polymerization (ROP) reaction of D,L-lactide; followed by a methacrylation reaction to form the macromonomer PLA-MA and a free radical polymerization to obtain the said graft copolymer. Also the nanoparticles resulting from the dialysis of said copolymer were successfully obtained. Each of the steps of the synthesis process gave rise to a product that was analyzed by ^{1}H-NMR spectroscopy and organic GPC analysis. Furthermore, after dialysis of the copolymer, an AFM analysis was also performed to obtain images of the synthesized nanoparticles, as well as a DLS analysis to determine the variation of particle size with temperature.

^{1}H-NMR spectra confirmed the formation of the nanoparticles. In fact, after dialysis, it was observed that the hydrophobic groups present in the ^{1}H-NMR spectrum of the copolymer were no longer visible. This is due to the fact that the hydrophobic groups, once they come into contact with water, are inverted, leaving the hydrophilic terminal groups on the outside of the nanoparticles.

DLS analysis resulted in an average nanoparticle size in the order of nanometers that was analyzed as a function of temperature. On the one hand, samples of nanoparticles dissolved in an acidic aqueous medium at pH at 37 ºC and 42 ºC were measured, in which a decrease in particle size was observed, as expected. On the other hand, a temperature ramp was carried out from 20 ºC to 45 ºC in which it was expected to obtain a decreasing trend in particle size. But certain stability was observed in terms of particle size with respect to the temperature, which may be due to the fact that the particles have not been formed correctly, or due to problems during the analysis.

The AFM analysis allowed obtaining the size of the nanoparticles, around a few hundred nanometers.

On the other hand, the functionalization of the HPMC was carried out to obtain the hydrogel in which the nanoparticles were encapsulated. The HPMC was functionalized in order to increase the interaction with the hydrophobic core of the nanoparticles. The hydrogel was analyzed by FT-IR analysis, SEM and rheological tests.

FT-IR analysis allowed obtaining the unique and characteristic IR spectrum of the HPMC-C_{12} hydrogel and comparing it with the non-functionalized HPMC.

Once the nanoparticles and the hydrogel had been characterized separately, by means of SEM analysis and rheological tests, the behavior of the system formed by the organic nanoparticles of PLA-g-P(NIPAm-co-MAA) with the HPMC-C_{12} hydrogel was verified.

SEM analysis provided micron-order high resolution images of the structure and appearance of the hydrogel. These images were obtained from the HPMC-C_{12} with and without nanoparticles. The main difference observed was in the appearance of the gel surface, with the gel without nanoparticles being smoother and the nanoparticles adhering to the gel being easily observed once introduced.

Regarding the rheological tests, an amplitude sweep test and a frequency sweep test were performed.

In the amplitude sweep, it was expected to find the limit value of the linear viscoelastic region (LVER) in which the elastic modulus (G') becomes less than the viscous modulus (G''). This test is necessary to determine the behavior of the gel. In contrast, a value of G'' higher than that of G' was obtained throughout the test, so the solid-like behavior of the gel could not be confirmed, but rather a liquid-like behavior.

Regarding the frequency sweep, a value of G' was again lower than that of G'' throughout the test, indicating that the material is not cross-linked.

The last tests carried out were those for the release of FITC as a drug simulator from the hydrogel-nanoparticle system. In this case, the cumulative percentage of FITC released from the system at 42 ºC was analyzed. This temperature was chosen to exceed the LCST of the copolymer that gave rise to the nanoparticles (37 ºC), which would determine the thermo and pH-responsive nature of the system.

After all the studies were carried out, a series of tests are interested to carry out as a future plan to complete this study.

First of all, it would be necessary to repeat the temperature ramp in the DLS to check if the nanoparticles are thermo-responsive. In addition, a drug release experiment with UV spectroscopy should be carried out to verify that the system works at 37 ºC, with the aim to compare it with the experiment done at 42 ºC and verify its thermo-responsiveness above 40 ºC; as well as to characterize the nanoparticles with the aim of verifying the LCST of the copolymer and their response when found in a medium at said temperature.

Another future goal to keep in mind would be with respect to rheological tests, trying to increase the concentration of particles in the hydrogel to obtain a less liquid behavior, or add more crosslinking agents, always ensuring the good injectability of the system.

Finally, once all these aspects of the hydrogel-nanoparticle system have been solved, the possibility of continuing the study with real drugs that are not simulators or increasing the temperature in the application to ensure efficient and successful localized drug release would be considered, for example utilizing gold nanoparticles which increase the localized temperature.

Bibliography

1. Hoare, T. R., & Kohane, D. S. (2008). Hydrogels in drug delivery: Progress and challenges. *Hydrogels in drug delivery: Progress and challenges*, 49(8), 1993–2007. https://doi.org/10.1016/j.polymer.2008.01.027

2. Raghuwanshi, V. S., & Garnier, G. (2019b). Characterisation of hydrogels: Linking the nano to the microscale. *Advances in Colloid and Interface Science*, 274, 102044. https://doi.org/10.1016/j.cis.2019.102044

3. Peppas, N., Hilt, J., Khademhosseini, A., & Langer, R. (2006). Hydrogels in Biology and Medicine: From Molecular Principles to Bionanotechnology. *Advanced Materials*, 18(11), 1345–1360. https://doi.org/10.1002/adma.200501612

4. Slaughter, B. V., Khurshid, S. S., Fisher, O. Z., Khademhosseini, A., & Peppas, N. A. (2009). Hydrogels in Regenerative Medicine. *Advanced Materials*, 21(32–33), 3307–3329. https://doi.org/10.1002/adma.200802106

5. Ganji, F., Vasheghani-Farahani,S., & Vasheghani-Farahani, E. (2010). Theoretical description of hydrogel swelling: a review. *Iranian polymer journal*, (5(119)),375-398. Https://www.sid.ir/en/journal/viewpaper.aspx?id=171784

6. Lin, C.C., & Metters, A.T. (2006). Hydrogels in controlled release formulations: Network design and mathematical modeling. *Advanced Drug Delivery Reviews*, 58(12–13), 1379–1408. https://doi.org/10.1016/j.addr.2006.09.004

7. Kabiri, K., Omidian, H., Hashemi, S., & Zohuriaan-Mehr, M. (2003). Synthesis of fast-swelling superabsorbent hydrogels: effect of crosslinker type and concentration on porosity and absorption rate. *European Polymer Journal*, 39(7), 1341–1348. https://doi.org/10.1016/s0014-3057(02)00391-9

8. Santoro, M., Marchetti, P., Rossi, F., Perale, G., Castiglione, F., Mele, A., & Masi, M. (2011). Smart Approach To Evaluate Drug Diffusivity in Injectable Agar−Carbomer Hydrogels for Drug Delivery. *The Journal of Physical Chemistry B*, 115(11), 2503–2510. https://doi.org/10.1021/jp1111394

9. Kim, S. W., Bae, Y. H., & Okano, T. (1992). Hydrogels: Swelling, Drug Loading, and Release. *Pharmaceutical Research*, 9(3)

10. Korsmeyer, R. W., Gurny, R., Doelker, E., Buri, P., & Peppas, N. A. (1983). Mechanisms of solute release from porous hydrophilic polymers. *International Journal of Pharmaceutics*, 15(1), 25–35. https://doi.org/10.1016/0378-5173(83)90064-9

11. Ionov, L. (2014). Hydrogel-based actuators: possibilities and limitations. *Materials Today*, 17(10), 494–503. https://doi.org/10.1016/j.mattod.2014.07.002

12. Kalagasidis Krušić, M., Ilić, M., & Filipović, J. (2009). Swelling behaviour and paracetamol release from poly(N-isopropylacrylamide-itaconic acid) hydrogels. *Polymer Bulletin*, 63(2), 197–211. https://doi.org/10.1007/s00289-009-0086-3

13. Klouda, L., & Mikos, A. G. (2015). Thermoresponsive hydrogels in biomedical applications. *European Journal of Pharmaceutics and Biopharmaceutics*, 97(68), 338–349. https://doi.org/10.1016/j.ejpb.2015.05.017

14. del Gado, E., de Arcangelis, L., & Coniglio, A. (2002). Critical dynamics at the sol–gel transition. *Physica A: Statistical Mechanics and its Applications*, 304(1–2), 93–102. https://doi.org/10.1016/s0378-4371(01)00513-1

15. Velada, J. L., Liu, Y., & Huglin, M. B. (1998). Effect of pH on the swelling behaviour of hydrogels based on N-isopropylacrylamide with acidic comonomers. *Macromolecular Chemistry and Physics*, 199(6), 1127–1134

16. Bukhari, S. M. H., Khan, S., Rehanullah, M., & Ranjha, N. M. (2015). Synthesis and Characterization of Chemically Cross-Linked Acrylic Acid/Gelatin Hydrogels: Effect of pH and Composition on Swelling and Drug Release. International *Journal of Polymer Science*, 2015, 1–15. https://doi.org/10.1155/2015/187961

17. Schmaljohann, D. (2006). Thermo- and pH-responsive polymers in drug delivery. *Advanced Drug Delivery Reviews*, 58(15), 1655–1670. https://doi.org/10.1016/j.addr.2006.09.020

18. Ullah, F., Othman, M. B. H., Javed, F., Ahmad, Z., & Akil, H. M. (2015). Classification, processing and application of hydrogels: A review. *Materials Science and Engineering: C*, 57, 414–433. https://doi.org/10.1016/j.msec.2015.07.053

19. Ahmed, E. M. (2015). Hydrogel: Preparation, characterization, and applications: A review. *Journal of Advanced Research*, 6(2), 105–121. https://doi.org/10.1016/j.jare.2013.07.006

20. Appel, E. A., Tibbitt, M. W., Webber, M. J., Mattix, B. A., Veiseh, O., & Langer, R. (2015). Self-assembled hydrogels utilizing polymer–nanoparticle interactions. *Nature Communications*, 6(1). https://doi.org/10.1038/ncomms7295

21. Guvendiren, M., Lu, H. D., & Burdick, J. A. (2012). Shear-thinning hydrogels for biomedical applications. *Soft Matter*, 8(2), 260–272. https://doi.org/10.1039/c1sm06513k

22. Grosskopf, A. K., Roth, G. A., Smith, A. A. A., Gale, E. C., Hernandez, H. L., & Appel, E. A. (2019). Injectable supramolecular polymer–nanoparticle hydrogels enhance human mesenchymal stem cell delivery. *Bioengineering & Translational Medicine*, 5(1). https://doi.org/10.1002/btm2.10147

23. Rossi, F., Santoro, M., Casalini, T., Veglianese, P., Masi, M., & Perale, G. (2011). Characterization and Degradation Behaviour of Agar–Carbomer Based Hydrogels for Drug Delivery Applications: Solute Effect. *International Journal of Molecular Sciences*, 12(6), 3394–3408. https://doi.org/10.3390/ijms12063394

24. Rossi, F., Chatzistavrou, X., Perale, G., & Boccaccini, A. R. (2011). Synthesis and degradation of agar-carbomer based hydrogels for tissue engineering applications. *Journal of Applied Polymer Science*, 123(1), 398–408. https://doi.org/10.1002/app.34488

25. Gao, W., Zhang, Y., Zhang, Q., & Zhang, L. (2016). Nanoparticle-Hydrogel: A Hybrid Biomaterial System for Localized Drug Delivery. *Annals of Biomedical Engineering*, 44(6), 2049–2061. https://doi.org/10.1007/s10439-016-1583-9

26. Lo, C. L., Lin, K. M., & Hsiue, G. H. (2005). Preparation and characterization of intelligent core-shell nanoparticles based on poly(d,l-lactide)-g-poly(N-isopropyl acrylamide-co-methacrylic acid). *Journal of Controlled Release*, 104(3), 477–488. https://doi.org/10.1016/j.jconrel.2005.03.004

27. Capella, V., Rivero, R.E., Liaudat, A.C., Ibarra, L.E., Roma, D.A., Alustiza, F., Mañas, F., Barbero, C.A., Bosch, P., Rivarola, C.R., & Rodriguez, N. (2019).

Cytotoxicity and bioadhesive properties of poly-N-isopropylacrylamide hydrogel. *Heliyon*, 5(4). https://doi.org/10.1016/j.heliyon.2019.e01474

28. Chung, J. E., Yokoyama, M., & Okano, T. (2000). Inner core segment design for drug delivery control of thermo-responsive polymeric micelles. *Journal of Controlled Release*, 65(1–2), 93–103. https://doi.org/10.1016/s0168-3659(99)00242-4

29. Singh, N. K., & Lee, D. S. (2014). In situ gelling pH- and temperature-sensitive biodegradable block copolymer hydrogels for drug delivery. *Journal of Controlled Release*, 193, 214–227. https://doi.org/10.1016/j.jconrel.2014.04.056

30. Brazel, C. S., & Peppas, N. A. (1996). Pulsatile local delivery of thrombolytic and antithrombotic agents using poly(N-isopropylacrylamide-co-methacrylic acid) hydrogels. *Journal of Controlled Release*, 39(1), 57–64. https://doi.org/10.1016/0168-3659(95)00134-4

31. NMR basic knowledge | Nuclear Magnetic Resonance Spectrometer (NMR) | Products | JEOL. (s. f.). Jeol. https://www.jeol.co.jp/en/products/nmr/basics.html

32. Aryal, S. (2022, 1 marzo). Gel Permeation Chromatography- Definition, Principle, Parts, Steps, Uses. Microbe Notes. https://microbenotes.com/gel-permeation-chromatography/

33. Edinburgh Instruments Ltd. (2020, 28 abril). UV Vis Spectroscopy | UV Vis *Spectroscopy Applications*. Edinburgh Instruments. https://www.edinst.com/techniques/uv-vis-spectroscopy/#:%7E:text=UV%2DVis%20Spectroscopy%20(or%20Spectrophotometry,a%20reference%20sample%20or%20blank

34. Penner, M. H. (2017). Ultraviolet, Visible, and Fluorescence Spectroscopy. *Food Science Text Series*, 89–106. https://doi.org/10.1007/978-3-319-45776-5_7

35. Stetefeld, J., McKenna, S. A., & Patel, T. R. (2016, septiembre). Dynamic light scattering: a practical guide and applications in biomedical sciences. Biophys Rev. https://doi.org/10.1007/s12551-016-0218-6

36. Pasquini, C. (2003). Near Infrared Spectroscopy: Fundamentals, Practical Aspects and Analytical Applications. J. Braz. Chem. Soc. https://www.scielo.br/j/jbchs/a/R8Z76mVbzwxk6RCYCLGkSnz/?format=pdf&lang=en

37. McIntyre, P. S., George, W. O., & Stuart, B. (2022). Modern Infrared Spectroscopy. Wiley India.

38. Widyatmoko, I. (2017). Sustainability of bituminous materials. *Sustainability of Construction materials*, 2.

39. Taffa, F. G. (2021). Thermo-responsive hydrogels for controlled drug delivery. Politecnico di Milano.

40. Atomic Force Microscopy (AFM) for Surface Topography analysis service. (2021, 19 abril). EAG Laboratories. https://www.eag.com/techniques/imaging/atomic-force-microscopy-afm/

41. Scanning electron microscopy (SEM). (2020, 24 august). Atria Innovation. https://www.atriainnovation.com/microscopia-electronica-de-barrido-sem-utilidades/

42. Joshi, S. C. (2011). Sol-Gel Behavior of Hydroxypropyl Methylcellulose (HPMC) in Ionic Media Including Drug Release. *Materials*, 4(10), 1861–1905. https://doi.org/10.3390/ma4101861

43. Lu, A., Petit, E., Wang, Y., Su, F., & Li, S. (2020). Synthesis and Self-Assembly of Hydroxypropyl Methyl Cellulose-block-Poly(ε-caprolactone) Copolymers as Nanocarriers of Lipophilic Drugs. ACS Applied Nano Materials, 3(5), 4367–4375. https://doi.org/10.1021/acsanm.0c00498

44. Akinosho, H., Hawkins, S., & Wicker, L. (2013). Hydroxypropyl methylcellulose substituent analysis and rheological properties. Carbohydrate Polymers, 98(1), 276–281. https://doi.org/10.1016/j.carbpol.2013.05.081

45. Lin, C. C., & Metters, A. T. (2006b). Hydrogels in controlled release formulations: Network design and mathematical modeling. *Advanced Drug Delivery Reviews*, 58(12–13), 1379–1408. https://doi.org/10.1016/j.addr.2006.09.004

46. Wang, Z., Liu, X., Duan, Y., & Huang, Y. (2021). Nanoparticle-Hydrogel Systems Containing Platensimycin for Local Treatment of Methicillin-Resistant Staphylococcus aureus Infection. Molecular Pharmaceutics, 18(11), 4099–4110. https://doi.org/10.1021/acs.molpharmaceut.1c00523

47. Lim, S. M., Oh, S. H., Lee, H. H., Yuk, S. H., Im, G. I., & Lee, J. H. (2010). Dual growth factor-releasing nanoparticle/hydrogel system for cartilage tissue engineering. Journal of Materials Science: Materials in Medicine, 21(9), 2593–2600. https://doi.org/10.1007/s10856-010-4118-1

List of Figures

List of Tables